

A NEW CLASS MESOPOROUS ALUMINOPHOSPHATES AS POTENTIAL
CATALYSTS IN THE UPGRADING PETROLEUM FEEDSTOCKS

FINAL TECHNICAL REPORT

REPORT PERIOD: SEPTEMBER 1, 2000 - FEBRUARY 31, 2005

PRINCIPAL INVESTIGATORS: CONRAD INGRAM, Ph. D. (PI)
MARK MITCHELL, Ph. D. (CO-PI)
PH: (404) 880-6898
FAX: (404) 880-6890
[Email: cingram@cau.edu](mailto:cingram@cau.edu)

SUBMITTED TO: U.S.DEPARTMENT OF ENERGY

REPORT DATE: AUGUST 31, 2005

GRANT NUMBER: DE-FG26-00NT40833

INSTITUTION: CLARK ATLANTA UNIVERSITY
223 JAMES P BRAWLEY DRIVE
ATLANTA, GA 30314

I ABSTRACT

A comprehensive investigation was conducted towards the synthesis and catalytic evaluation of high surface areas, uniform pore size, mesoporous aluminophosphates (AlPO_4) as potential catalysts for the upgrading of heavy petroleum feedstock, such as heavy crudes and petroleum residuum. The influence of several synthesis variables (including, the nature of the reactants, chemical composition of reaction mixtures, time and temperature) on the synthesis and physicochemical characteristics of the resulting products was explored. Phosphoric acid and three different aluminum sources, namely, aluminum hydroxide, aluminum isopropoxide and pseudoboehmite alumina, were used as the inorganic precursors. Cetyltrimethylammonium chloride (C_{16}TACl) surfactant was used as charge compensating cation and structure directing agent in the surfactant-micellar-mediated synthesis pathway employed. Synthesis were conducted from reaction mixtures within the following typical molar composition range: $x\text{Al}_2\text{O}_3:\text{P}_2\text{O}_5:y\text{C}_{16}\text{TACl}:z\text{TMAOH}:w\text{H}_2\text{O}$, where $x = 0.29\text{-}2.34$, $y = 0.24\text{-}0.98$, $z = 0.34\text{-}1.95$, $w = 86\text{-}700$. Selected materials were evaluated for the conversion of isopropylbenzene (cumene) in order to understand the nature of any acid sites created. The synthesis products obtained depended strongly on the molar composition of the synthesis mixture. A lamellar (layered) phase was favored by synthesis mixtures comprised of low Al/P ratios (<0.33), low TMAOH content, high C_{16}TACl concentrations and high synthesis temperature (110°C). Formation of the desired hexagonal (tubular) phase was favored by higher Al/P ratios and TMAOH content, pH range between 8-10, low C_{16}TACl concentration and ambient temperature. The aluminum source had significant influence on the products obtained. With aluminum hydroxide ($\text{Al}(\text{OH})_3$) as the hydroxide source, the resulting hexagonal phase in the "as-synthesized" form demonstrated well defined ordered mesoporous structure for synthesis mixtures of Al/P ratios in the range of 0.47-1.25, above which increasingly disordered products were observed. The products were however unstable to calcination in air above 400°C to remove the organic template, under which structural collapsed was observed. Products formed using pseudoboehmite alumina (catapal B), were more thermally stable than those formed with aluminum isopropoxide, though all products experienced some degree of structural collapsed on calcination and yielded micro- or micro-mesoporous materials ranging from low ($<500\text{ m}^2/\text{g}$) to high surface areas ($>500\text{ m}^2/\text{g}$) and pore sizes ranging from microporous ($< 1.5\text{ nm}$) in some products to mesoporous (up to 3.6 nm) in other. Improvement in thermal stability was not observed when Mg and Co or bridging organic functional groups were incorporated with the mesoporous framework. The products showed negligible activity for the conversion of cumene at 300°C . Further research is necessary to investigate alternative synthesis strategies to strengthen and improve the thermal stabilities of these aluminophosphates .

II. DISCLAIMER

This report was prepared as an account of work sponsored by an agency of the United States Government. Neither the United States States Government nor any agency thereof, nor any of their employees, makes any warranty, express or implied, or assumes any legal liability or responsibility for the accuracy, completeness, or usefulness of any information, apparatus, product, or process disclosed, or represents that its use would not infringe privately owned rights. Reference herein to any specific commercial product, process, or service by trade name, trademark, manufacturer or otherwise does not necessarily constitute or imply its endorsement, recommendation, or favoring by the United States Government or any agency thereof. The views and opinions of authors expressed herein do not necessarily state or reflect those of the United States Government or any agency thereof.

III. EXECUTIVE SUMMARY

Increasing demand for processing heavy petroleum feedstocks (containing 10-30% residue) to high quality transportation fuels has heightened the importance to develop new highly active and deactivation resistant catalyst systems with large pores sizes, high surface areas, good thermal stability and access to catalytic sites. Thus, this project was focused on exploring the synthesis of inorganic mesoporous aluminophosphates (AlPO_4) for application in the acid catalyzed conversion of large petroleum feedstock compounds to useful middle distillates and naphtha transportation fuels. Summarized herein, is the outcome of our research for the project period for September 1, 2000 to February 29, 2005. A systematic study of the influence of several variables (gel composition, synthesis techniques, synthesis time and temperature) on the synthesis and physicochemical characteristics (including catalytic activities) on mesoporous (AlPO_4) was conducted. Selected materials were evaluated on the conversion of isopropylbenzene (cumene) to understand the nature of any acid sites created. In general, syntheses were conducted by combining aluminum and phosphorus precursors, cetyltrimethylammonium chloride (CTACl) as surfactant, tetramethylammonium hydroxide (TMAOH) and water with typical molar composition of the synthesis mixture as follows: $x\text{Al}_2\text{O}_3 : \text{P}_2\text{O}_5 : 0.5\text{CTACl} : 2.6\text{TMAOH} : 351\text{H}_2\text{O}$, where $x = 0.29-2.34$. A variety of hexagonal and lamellar AlPO_4 with pores size distribution in the $20\text{\AA}-40\text{\AA}$ range were prepared in the presence of long chain CTACl surfactant. The products obtained depended on the molar composition of the synthesis mixture. The aluminum source had significant influence on the products obtained. Products formed using pseudoboehmite alumina (catapal B), were more thermally stable than those formed with aluminum isopropoxide. Aluminum hydroxide gave thermally unstable products. Lamellar phase was favored by extremely low Al/P ratios (<0.33), low TMAOH content, high C_{16}TACl concentrations and high synthesis temperature (110°C). The hexagonal phase was favored by higher Al/P ratios and TMAOH content, pH range between 8-10, low C_{16}TACl concentration and ambient temperature. With $\text{Al}(\text{OH})_3$ as the hydroxide source, the hexagonal phase demonstrated highest lattice ordering at Al/P ratios 0.47-1.25, above which increasingly disordered products were observed. Mesoporous aluminophosphates synthesized as pure AlPO_4 or with organosilanes as components of the ordered structures (added during condensation) maintained mesoporous structures, high surface areas up to $600\text{ m}^2/\text{g}$ and pore volume and uniform pore sizes up to 36\AA , after calcination in nitrogen only up to 350°C , beyond which their

structures collapsed into amorphous materials. Products formed using pseudoboehmite alumina (catapal B), were more thermally stable than those formed with aluminum isopropoxide, though all products experienced some degree of structural collapse on calcination and yielded micro- or micro-mesoporous materials ranging from low (<500 m²/g) to high surface areas (>500 m²/g) and pore sizes ranging from microporous (< 1.5 nm) in some products to mesoporous (up to 3.6 nm) in other. The pore sizes were affected by the water content of the synthesis mixtures. Improvement in thermal stability was not observed when Mg and Co or bridging organic functional groups were incorporated with the mesoporous framework. The products showed negligible activity for the conversion of cumene at 300°C. Further research is necessary to investigate alternative synthesis strategies to strengthen and improve the thermal stabilities of these aluminophosphates .

TABLE OF CONTENTS

	Page
I ABSTRACT.....	ii
II DISCLAIMER.....	iii
III EXECUTIVE SUMMARY	iv
LIST OF FIGURES	ix
LIST OF TABLES	xii
LIST OF SCHEMES	xiii
LIST OF ABBREVIATIONS	xiv
1: INTRODUCTION AND PROJECT OBJECTIVES.....	1
2. BACKGROUND	2
3: EXPERIMENTAL DETAILS.....	5
3.1 Materials	5
3.2 Synthesis.....	6
3.2.1 Synthesis of aluminophosphates using aluminum hydroxide	6
3.2.1.1 Effect of the Al/P ratio.....	6
3.2.1.2 Effect of the amount of TMAOH	6
3.2.1.3 Effect of the amount of CTACl.....	7
3.2.1.4 Effect of synthesis time	7
3.2.1.5 Effect of mixing time of aluminium and phosphorous precursors	7
3.2.2 Synthesis of aluminophosphates using aluminum isopropoxide.....	7
3.2.2.1 Effect of Al/P ratio and mixing time	7
3.2.2.2 Effect of TMAOH concentration.....	8

3.2.2.3	Effect of CTACl concentration.....	8
3.2.2.4	Effect of water concentration.....	8
3.2.3	Synthesis of aluminophosphates using Psuedobohemite alumina.....	9
3.2.3.1	Effect of Al/P ratio.....	9
3.2.3.2	Effect of water concentration.....	9
3.2.4	Synthesis of cobalt and magnesium and organic containing aluminophosphates.....	9
3.3	Calcination.....	10
3.4	Characterization.....	10
3.4.1	X-ray powder diffraction.....	10
3.4.2	Surface area and pore size distribution analysis.....	10
3.4.3	Thermogravmetric analysis.....	11
3.4.4	Magic angle spinning NMR analysis.....	11
3.4.5	Chemical analysis by ICP-MS.....	11
3.4.6	Infrared Spectrometry.....	12
3.5	Catalytic Testing.....	12
4.	RESULTS AND DISCUSSION.....	12
4.1	Synthesis of aluminophosphate with aluminium hydroxide.....	13
4.1.1	Effect of Al/P ratio.....	18
4.1.2	Effect of TMAOH concentration.....	24
4.1.3	Effect of surfactant concentration.....	33
4.1.4	Effect of synthesis time.....	35
4.1.5	Effect of mixing time.....	38

4.2 Effect of aluminum source	41
4.2.1 Synthesis of mesoporous aluminophosphates using aluminum	41
4.2.1.1 Effect of Al/P ratio	41
4.2.1.2 Effect of TMAOH concentration	46
4.2.1.3 Effect of surfactant concentration	48
4.2.1.4 Effect of water concentration	49
4.3 Synthesis of mesoporous aluminophosphates using psuedobohemite alumina	55
4.3.1 Effect of A/P ratios	56
4.3.2 Effect of water concentration	60
4.4 Synthesis of Aluminophosphate containing Mg and Cob	65
4.5 Catalytic Testing	69
5: CONCLUSIONS	70
6. FUTURE WORK	71
7 . PRESENTATION AND PUBLICATIONS	71
8.. REFERENCES	72

LIST OF FIGURES

FIGURE	PAGE
1 XRD Patterns of a) Lamellar and b) Hexagonal phase	14
2 ²⁷ Al and ³¹ P MAS NMR of Hexagonal (Al/P=0.58) and Lamellar phase (Al/P=0.58)	15
3 IR spectrum of a) Lamellar b) Hexagonal phase	16
4 TGA/DTA data of a) Lamellar and b) Hexagonal phase	18
5 XRD patterns of patterns of samples synthesized at various Al/P ratios in mixture.....	20
5B. Thermograms of mesoporous aluminophosphates synthesized under various Al/P ratio.....	21
6 XRD data of a) As-synthesized and b) Calcined sample synthesized at Al/P of 1.25.....	23
7 XRD patterns of products obtained from synthesis mixtures of various TMA/P ₂ O ₅ ratios and fixed Al/P of 0.58 (synthesis conducted at 25°C).....	25
8 XRD patterns of products obtained from synthesis mixtures of various TMA/P ₂ O ₅ ratios and fixed Al/P of 0.58 (synthesis conducted at 110°C).....	26
9 XRD patterns of products obtained from synthesis mixtures of various TMA/P ₂ O ₅ ratios and fixed Al/P of 1.17 (synthesis conducted at 25°C).....	27
10 XRD patterns of products obtained from synthesis mixtures of various TMA/P ₂ O ₅ ratios and fixed Al/P of 1.17 (synthesis conducted at 110°C).....	29
11 XRD patterns of products obtained from synthesis mixtures of various TMA/P ₂ O ₅ ratios and fixed Al/P of 1.77 (synthesis conducted at 25°C).....	30
12 XRD patterns of products obtained from synthesis mixtures of various TMA/P ₂ O ₅ ratios and fixed Al/P of 1.77 (synthesis conducted at 110°C)	32
13 XRD patterns of products obtained from synthesis mixtures of various CTACl/P ₂ O ₅ ratios and fixed Al/P of 0.58 (synthesis conducted at 25°C).....	34
14 XRD patterns of products obtained from synthesis mixtures of various CTACUP205 ratios and fixed AUP of 0.58 (synthesis conducted at 110°C).....	35
15 XRD patterns obtained at various reaction mixture times and fixed Al/P of 0.58 (0.5hrs mixing before TMAOH addition).....	36

16	XRD patterns obtained at various reaction mixture times and fixed Al/P of 0.58 (2hrs mixing before TMAOH addition)	37
17	XRD patterns of the effect of mixing time before TMAOH addition at a fixed Al/P of 0.58 and 1.17 (synthesis conducted at 25°C)	38
18	a) Adsorption isotherm and b) pore size distribution of calcined samples synthesized from various mix time at a fixed Al/P of 0.58.....	39
19	a) Adsorption isotherm and b) pore size distribution of calcined samples synthesized from various mix time at a fixed Al/P of 1.17	40
20	XRD patterns of patterns of samples synthesized at various AUP ratios in mixture at 25°C	41
21	a) Adsorption isotherm and b) pore size distribution of calcined samples synthesized at various Al/P ratios (2hrs mixing before TMAOH addition).....	42
22	a) Adsorption isotherm and b) pore size distribution of calcined samples synthesized at various Al/P ratios (6hrs mixing before TMAOH addition).....	45
23	XRD patterns of products obtained from synthesis mixtures of various TMA/P ₂ O ₅ ratios and Al/P of 0.59 (synthesis conducted at 25°C)	47
24	XRD patterns of products obtained from synthesis mixtures of various TMA/P ₂ O ₅ ratios and Al/P of 1.17 (synthesis conducted at 25°C)	47
25	XRD patterns of products obtained from synthesis mixtures of various CTACl/P ₂ O ₅ ratios and fixed Al/P of 0.58 (synthesis conducted at 25°C 110°C)	49
26	XRD patterns of products obtained from synthesis mixtures of various CTACl/P ₂ O ₅ ratios and fixed Al/P of 1.16 (synthesis conducted at 25°C and 110°C)	50
27	XRD patterns of products obtained from synthesis mixtures of various H ₂ O/P ₂ O ₅ ratios and fixed Al/P of 0.58 (synthesis conducted at 25°C)	52
28	XRD patterns of products obtained from synthesis mixtures of various H ₂ O/P ₂ O ₅ ratios and fixed Al/P of 1.15 (synthesis conducted at 25°C)	53
29	a) Adsorption isotherm and b) pore size distribution from synthesis mixtures of various H ₂ O/P ₂ O ₅ ratios and fixed Al/P of 0.58 (synthesis conducted at 25°C)	54
30	a) Adsorption isotherm and b) pore size distribution from synthesis mixtures of various H ₂ O/P ₂ O ₅ ratios and fixed Al/P of 1.15 (synthesis conducted at 25°C).....	55
31	XRD patterns of patterns of samples synthesized at various Al/P ratios in	

	mixture (synthesis conducted at 25°C).....	57
32	a) Adsorption isotherm and b) pore size distribution of calcined samples synthesized at various Al/P ratios in mixture (synthesis conducted at 25°C).....	58
33	XRD patterns of patterns of samples synthesized at various Al/P ratios in mixture (synthesis conducted at 110°C)	59
34	Adsorption isotherm of calcined samples synthesized at various Al/P ratios in mixture (synthesis conducted at 110°C)	60
35	a) Adsorption isotherm and b) pore size distribution from synthesis mixtures of various H ₂ O/P ₂ O ₅ ratios and fixed Al/P of 1.17 (synthesis conducted at 25°C).....	62
36	a) Adsorption isotherm and b) pore size distribution from synthesis mixtures of various H ₂ O/P ₂ O ₅ ratios and fixed Al/P of 0.58 (synthesis conducted at 25°C)	
37	a) Adsorption isotherm and b) pore size distribution from synthesis mixtures of various H ₂ O/P ₂ O ₅ ratios and fixed Al/P of 1.17 (synthesis conducted at 110°C)...	64
38	a) Adsorption isotherm and b) pore size distribution from synthesis mixtures of various H ₂ O/P ₂ O ₅ ratios and fixed Al/P of 0.58 (synthesis conducted at 110°C)	65
39	XRD of “As-synthesized” cobalt containing mesostructured AlPO sample.....	66
40	Adsorption-desorption isotherms of calcined cobalt containing mesostructured AlPO ₄ sample.....	66
41	Adsorption-desorption isotherms of calcined mesoporous organo-aluminumphosphate synthesized in the presence of propyltriethoxysilane.....	67
42	Adsorption-desorption isotherms of calcined mesoporous organo-aluminumphosphate synthesized in the presence of 3-aminopropyltriethoxysilane.....	68
43	dsorption-desorption isotherms of calcined mesoporous organo-aluminumphosphate synthesized in the presence of 1,2 bis-trimethoxysilylthane.....	68

LIST OF TABLES

Table 1	Effect of Al/P composition of starting mixtures on Al/P ratio in products.....	19
Table 2.	Weight loss events from TGA Analysis of mesoporous aluminophosphates.....	22

LIST OF SCHEMES

Scheme 1:	Representation of the arrangement of AlPO_4 structural framework.....	3
Scheme 2	Pictorial of catalytic reactor	12

LIST OF ABBREVIATIONS/ACRONYMS

MCM-41	Mobil Composite Material-41
SBA-15	Santa Barbara-15
TMAOH	Tetramethylammonium hydroxide
CTACl	Cetyltrimethylammonium chloride
XRD	X-ray Diffraction Spectrometry
TGA	Thermogravemetric Analysis
DTA	Differential Thermogravemetric Analysis
ICP-MS	Inductively Coupled Plasma Mass Spectrometry
MAS-NMR	Magic Angle Spining Nuclear Magnetic Resonance
BET	Braunner, Emmett and Teller
BJH	Barrett, Joyner and Halenda
AlPO ₄	Aluminophosphat

1. INTRODUCTION AND PROJECT OBJECTIVES

Increasing demand for processing heavy petroleum feedstock has heightened the importance of developing new catalyst systems. Many conventional crude oils from around the world contain 10-30% residue (which is the fraction of crude oil with boiling point greater than 525°C). As conventional crude oils have become more expensive, interest in processing heavier feeds has increased. These heavier feeds have residue contents of 40% or more, and require further processing in order to find a market. The current motivations for conversion technologies are multifold. The market for heavier fuels is decreasing while that for middle distillate is increasing at a rapid rate.¹ In many parts of the world, light oil production is declining and heavy oil conversion, therefore, becomes increasingly important to maintain economic viability of these regions. Further tightening of environmental in the United States has provided incentives to refiners to further reduce sulfur and aromatic levels of the finished products. Additional stringent requirements on the disposal of refinery residues such as coke or residue encourage “minimum-waste” refinery strategies.

To process heavy feedstock, the catalysts of use must possess high surface area, Bronsted acidic properties, as well as thermal stability. Zeolites and other catalysts have been encountering a growing interest due to their critical applications in petroleum refining. Therefore, there are research efforts in trying to synthesize new kinds of zeolite-type materials. Zeolites possess high acidity, high surface area and a rigid 3-dimensional framework structure. These properties make them useful for petroleum processing. Zeolites, however, often suffer from diffusion limitation and their uses are therefore limited to petroleum fractions containing small substrates with kinetic diameters less than 8Å. Because of these limitations, a myriad of synthetic efforts are being conducted to design catalysts with enlarged pore sizes.²

In the early 1980's, Union Carbide Laboratories reported a new generation of zeolite-like microporous materials, the aluminophosphates. The aluminophosphates (AlPO₄) with open network structure were synthesized using similar template molecules as in zeolite synthesis. This represented a significant advancement in the field of porous materials as these materials contained similar framework topologies as those found in zeolites but differed in chemical composition. Their applications as catalysts were restricted, since the neutral framework was lacking in acidic characteristic. These porous aluminophosphate molecular sieves are known to

exist in a wide range of structural and compositional diversity, and are generally prepared from gels containing aluminum, phosphorous and an amine acting as a structure-directing agent. The addition of silicon and other metals to the framework resulted in the silicoaluminophosphate (SAPO) and metal substituted aluminophosphates (MeAPO).³ The substitution of divalent metal ions in the framework of an aluminophosphate molecular sieve imparts acidity, redox characteristics, ion-exchange capacity and enhanced hydrophilicity with greater stability, structural and chemical diversity.⁴

In the quest for high surface area catalysts with greater stability, structural and chemical diversity, large pore size materials in the mesoporous range denoted as M41S aluminosilicate were invented by Mobil researchers in 1992.⁵ MCM-41, a member of this series, possesses a regular array of uniform and one-dimensional mesopores that can be tuned to the desired pore diameter in the range of 20Å. The use of surfactants plays an extremely important role in the synthesis of these solids due to a self-assembly process, known as the liquid crystal templating mechanism (LCT), to form the mesoporous materials. Following the successful synthesis of MCM-41, it is instructive that the synthesis of the mesoporous aluminophosphate counterparts be investigated. Mesoporous aluminophosphates are expected to retain the physiochemical characteristics of their microporous counterparts, but with significant increase in pore size, pore volume and surface area. Few researchers have explore the synthesis of aluminophosphate, but pathways to the successful synthesis of these potential catalysts remain unclear.

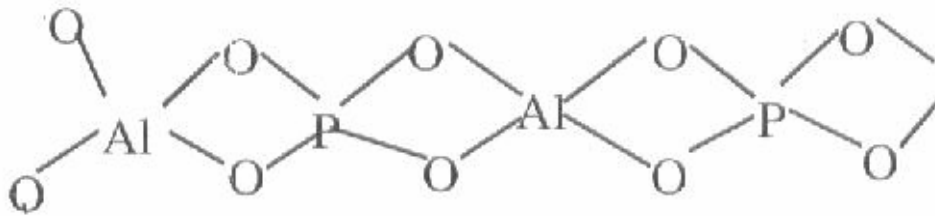
Project Objectives

This project was focussed on synthesizing the aluminophosphates for use as catalysts in petroleum upgrading and to comprehensively investigate the effect of reaction parameters such as the amount of TMAOH, Al/P ratio and water content as well as reaction temperature and time on their synthesis and catalytic properties.

2. BACKGROUND

Aluminophosphate inorganic framework composed of Al³⁺ or P⁵⁺ is based on the assemblage of aluminate and phosphate species as indicated in Scheme 1. A notable feature of the microporous AlPO₄ composition is the invariant Al₂O₃/ P₂O₅ ratio, which is in direct contrast with the variable

compositions of $\text{SiO}_2/\text{Al}_2\text{O}_3$ ratio found in the aluminosilicate zeolite counterparts. Whereas zeolites contain Al^{3+} and Si^{4+} in the tetrahedral coordination and exhibit a net negative framework charge, the AlPO_4 materials may contain aluminum in coordination other than tetrahedral and a framework that is neutral, as well as Bronsted acid sites caused by the presence of terminal-OH bonds on the external surface of the crystal.



Scheme 1: Representation of the arrangement of AlPO_4 structural framework

The overall composition of the AlPO_4 molecular sieves is written as: $x\text{R}:\text{Al}_2\text{O}_3:\text{P}_2\text{O}_5: y\text{H}_2\text{O}$, where R is an organic amine or quaternary ammonium ion. The quantities x and y represent the amount of organic or water that fills the pores of the crystal. Just as the zeolites obey Lowenstien's rule for the avoidance of tetrahedral Al-O-Al groupings within the structure, the AlPO_4 structures avoid forming tetrahedral Al-O-Al bonds as well as P-O-P bonds.

Phosphate based molecular sieves are normally synthesized from initially acidic gels containing organic additives in an aqueous medium. It is well known that the choice of aluminum source plays a crucial role in the synthesis and phase purity of AlPO_4 molecular sieves. Moreover, parameters such as temperature, duration of crystallization and agitation will also affect the crystallization of the molecular sieves. The synthesis of aluminophosphate therefore normally takes place by the following steps: neutralization of the Al source suspended in water with a nearly equimolar amount of dilute phosphoric acid to obtain the reactive AlPO_4 gel, aging of the reactive gel, addition of a particular organic additive to the reactive gel referred to as the precursor gel, and aging of the precursor gel. Aluminum species can exist in solution in a

number of forms:

- 1) hydrated octahedral Al^{3+}
- 2) polymeric octahedral AlO_6
- 3) mixed $\text{AlO}_4/\text{AlO}_6$ species
- 4) polymeric AlO_4
- 5) isolated $\text{Al}(\text{OH})_4^-$ and various deprotonated forms

After the successful synthesis of the hexagonal and cubic members of the ordered mesoporous materials, further research efforts led to a wide range of other structures, such as the well ordered hexagonal mesoporous silica structures (SBA-15) with uniform pore sizes up to approximately 300 Å. Prior to the discovery of these materials, the mesoporous silicas were limited to 100 Å and had wall thicknesses around 10 Å.⁸ The use of triblock copolymer surfactants, for example, poly(alkylene)oxide ($\text{EO}_5\text{PO}_7\text{EO}_5$) expands the wall thickness up to 60 Å and gives substantially higher pore sizes up to 300 Å.⁶

Based on the catalytic success of zeolites and the great catalytic potential of microstructured aluminophosphates and the mesostructured M41S family, numerous attempts have been made to prepare mesostructured aluminophosphates but with inconsistent results. Sayari *et al.* reported the use of dodecylamine surfactant as a structure directing agent to synthesize mesoporous aluminophosphates at 100 °C and 24 hours reaction conditions, which resulted in a lamellar phase.⁷ Calcination of the lamellar material at 400 °C under flowing nitrogen followed by a flow of air resulted in a collapse of the lamellar structure. The organic moiety, in addition, could not be removed by solvent extraction. A lamellar aluminophosphate phase was also reported by Klinowki *et al.* using a cationic surfactant templating agent.⁸ Reaction temperatures employed ranged from 80-150 °C for 24-96 hours. Upon calcinations at 250 °C, an amorphous product was similarly obtained.²⁸ Yue *et al.* also reported the synthesis of lamellar aluminophosphates using a mixture of ethylene glycol and an unbranched primary alcohol as the medium and hexylamine as the template. The mixtures were kept at 180 °C for 8 days.⁹ Using dodecylphosphate as a template Tiemann *et al.* also reported the synthesis of lamellar aluminophosphates. The mixture was kept at 120 °C for 24 hours without agitation.¹⁰ Ozin and coworkers also reported the synthesis of lamellar aluminophosphate under solvothermal conditions using primary alkyl amines in tetraethylene glycol.¹¹ On the other hand, Stucky and coworkers prepared the

hexagonal phase by adding phosphoric acid and hydrofluoric acid to aluminum isopropoxide in ethanol, followed by cetyltrimethylammonium bromide (CTAB) at room temperature. Placing the gel in an oven at 70⁰C for a few days led to a partial conversion of a lamellar to hexagonal phase. Attempts to calcine the products into a mesoporous structure resulted in structural collapse.¹²

Kevan *et al.* reported the room temperature synthesis of a partially stable hexagonal aluminophosphate using CTAC1 as templating agent and aluminum hydroxide as the aluminum source.¹³ Kimura *et al.* reported that synthesis conducted at 130⁰C for 5 days resulted in a lamellar mesostructure. A hexagonal phase was however, obtained only when the liquid mixture was dispersed in distilled water.¹⁴ Thermally stable microporous/mesoporous aluminophosphates with continuously adjustable pore sizes prepared at 160⁰C and cooled to 120⁰C using Al(OBut)₃ and triethanolamine through the surfactant (CTAB) assisted procedure was reported.¹⁵ In addition, silicoaluminophosphate synthesis based on a self assembly process using CTAC1, tetraorthosilicate (TEOS) and aluminum hydroxide at room temperature was also reported.¹³

Project Objectives

Factors leading to successful synthesis of aluminophosphates remained unclear. This project was focussed on synthesizing the aluminophosphates for use as catalysts in petroleum upgrading and to comprehensively investigate the effect of reaction parameters such as the amount of TMAOH, Al/P ratio and water content as well as reaction temperature and time on their synthesis and catalytic properties.

3. EXPERIMENTAL DETAILS

MATERIALS AND METHODS

3.1 Materials

Hexadecyltrimethylammonium chloride [C₁₆H₃₃(CH₃)₃NCl, C₁₆TMACl, 25 wt in water, Aldrich Chemical Co], tetramethylammonium hydroxide [(CH₃)₄NOH, TMAOH, 25 wt % in water, Aldrich Chemical Co.], aluminum isopropoxide [(CH₃)₂CHO]₃Al, 98% Aldrich Chemical Co.], aluminum hydroxide hydrate [Al(OH)₃H₂O, Aldrich Chemical Co.], Pseudoboehmite alumina

[Al(OH)₃, Vista Chemical Co.], O-Phosphoric acid, 85% H₃PO₄, Fischer Scientific], magnesium nitrate hexahydrate, cobalt acetate.

3.2. Synthesis

3.2.1 Synthesis of aluminophosphates using aluminum hydroxide

Aluminum hydroxide source has successfully been used for synthesis of microporous aluminophosphates. This research therefore utilized aluminium hydroxide as the initial source of aluminum. Several parameters that affect the synthesis are investigated.

In typical synthesis, 3.53g aluminum hydroxide was slowly added to a solution of 4.2g phosphoric acid in 15 ml water under vigorous stirring. The mixture was added to a solution of 11.6g CTACl in 100 ml water with vigorous stirring. After 0.5hr, 17.3g of TMAOH was slowly added drop-wise and a wet gel was obtained. The final mixture was then divided into two aliquots. One aliquot was stirred for 24 hr at 25°C. The second was heated at 110°C under static conditions.

3.2.1.1 Effect of the Al/P ratio

Six synthesis mixtures were prepared as in Section 3.2, but each with different amounts of aluminum hydroxide as follows: 0.83,0.95,1.33,1.66,3.59 and 6.66g. The molar composition of the reaction mixtures were as follows: $x\text{Al}_2\text{O}_3:\text{P}_2\text{O}_5:0.50\text{C}_{16}\text{TACl}:2.60\text{TMAOH}:350\text{H}_2\text{O}$ where $x = 0.29-2.34$. The reaction mixtures were allowed to react for 72 hr and were otherwise treated as in Section 3.2.

3.2.1.2 Effect of TMAOH concentration

Reaction mixtures with three different Al/P ratios (0.58, 1.17 and 1.77) were used for this experiment. For each Al/P ratio, five synthesis mixtures, each with different amounts of TMAOH, were prepared as follows: 7.40,9.87,14.64,22.96 and 24.39g of TMAOH for Al/P ratio= 0.58; 5.3, 8.8,15.7,20.0 and 22.4g of TMAOH for Al/P ratio= 1.17; and, 4.5,7.6,15.4, 20.8 and 26.0g of TMAOH for Al/P ratio= 1.77. The molar composition of the reaction mixtures were as follows:

(1) $0.58\text{Al}_2\text{O}_3:\text{P}_2\text{O}_5:0.50\text{C}_{16}\text{TMACl}:x\text{TMAOH}:347\text{H}_2\text{O}$, where $x = 0.53-1.82$

(2) $1.17\text{Al}_2\text{O}_3:\text{P}_2\text{O}_5:0.50\text{C}_{16}\text{TMACl}:y\text{TMAOH}:344\text{H}_2\text{O}$, where $y = 0.39-1.68$

(3) $1.77\text{Al}_2\text{O}_3:\text{P}_2\text{O}_5:0.50\text{C}_{16}\text{TMACl}:z\text{TMAOH}:350\text{H}_2\text{O}$, where $z = 0.34-1.40$

The reaction mixtures were otherwise treated as in Section 3.2.

3.2.1.3 Effect of CTACl concentration

The Al/P ratio chosen for this experiment was 0.58. Four synthesis mixtures were prepared each with the following weight of CTACl: 5.8, 8.0, 17.0 and 23.2g. The molar composition of the reaction mixtures were as follows: $0.58\text{Al}_2\text{O}_3:\text{P}_2\text{O}_5:y\text{C}_{16}\text{TACl}:3.44\text{TMAOH}:348\text{H}_2\text{O}$, where $y = 0.24-0.98$. The reaction mixtures were otherwise treated as in Section 3.2.

3.2.1.4 Effect of synthesis time

Six identical reaction mixtures with molar composition of $0.58\text{Al}_2\text{O}_3:\text{P}_2\text{O}_5:0.50\text{C}_{16}\text{TACl}:3.22\text{TMAOH}:350\text{H}_2\text{O}$ were prepared as per section 3.2. The mixtures were allowed to react and one sample was analyzed after each of the following synthesis time: 5, 10, 24, 48, 72 and 96 hr.

3.2.1.5 Effect of mixing time of aluminum and phosphorous precursors

The experiment was done to investigate the effect of mixing time of aluminum and phosphorous precursors on the product obtained. Reaction mixtures with two Al/P ratios (0.58 and 1.17) were used with molar composition of the starting mixtures as follows:

(1) $0.58\text{Al}_2\text{O}_3:\text{P}_2\text{O}_5:0.50\text{C}_{16}\text{TACl}:3.02\text{TMAOH}:349\text{H}_2\text{O}$

(2) $1.17\text{Al}_2\text{O}_3:\text{P}_2\text{O}_5:0.50\text{C}_{16}\text{TMACl}:2.68\text{TMAOH}:349\text{H}_2\text{O}$

Aluminum and phosphorous precursors were mixed for 0.5, 2, 4, and 6 hr prior to the addition of TMAOH. The synthesis time was at 72 hr at 25°C . The reaction mixtures were otherwise treated as in Section 3.2.

3.2.2. Synthesis of aluminophosphates using aluminum isopropoxide

The synthesis procedure was as per section 3.2.1 except that aluminum isopropoxide was used as the aluminum source.

3.2.2.1 Effect of the Al/P ratio and mixing time

Four synthesis mixtures, differing only in the amounts of aluminum isopropoxide, were

prepared. Aluminum isopropoxide weights were as follows: 4.4, 5.8, 8.7 and 17.5g. The molar composition of the synthesis mixtures were as follows:

$x\text{Al}_2\text{O}_3:\text{P}_2\text{O}_5:0.50\text{C}_{16}\text{TACl}:1.5\text{TMAOH}:349\text{H}_2\text{O}$, where varied from 0.58 to 2.33. A 6 hr mixing of aluminum and phosphorous species was also conducted before the addition of TMAOH. The synthesis mixtures were otherwise treated as in Section 3.2.

3.2.2.2 Effect of TMAOH concentration

TMAOH variation on each of two reaction mixtures of different Al/P ratios (0.59 and 1.17) were conducted. For the 0.59 Al/P ratio mixture, 2.88, 3.46 and 7.22g of TMAOH was added, while for the 1.17 Al/P ratio mixture, 0.0, 2.18 and 20.4g of TMAOH were added. The molar composition of the mixtures obtained were as follows:

(1) $0.58\text{Al}_2\text{O}_3:\text{P}_2\text{O}_5:0.50\text{C}_{16}\text{TACl}:x\text{TMAOH}:347\text{H}_2\text{O}$, where $x = 0.53-1.82$

(2) $1.17\text{Al}_2\text{O}_3:\text{P}_2\text{O}_5:0.50\text{C}_{16}\text{TACl}:x\text{TMAOH}:349\text{H}_2\text{O}$, where $x = 0.34-1.95$

In addition to synthesis at 25°C separate aliquots of the mixtures were also subjected to a higher temperature (110°C). The mixtures were otherwise treated in the same manner as in Section 3.2.

3.2.2.3 Effect of CTACl concentration

Three CTACl variations on each of two reaction mixtures of different Al/P ratios (0.58 and 1.16) were prepared. For mixtures with Al/P ratio= 0.58, the CTACl weights were 5.80, 7.74 and 17.4g while for mixtures with Al/P ratio=1.16, the weights were 5.80, 7.75 and 17.4g. The molar compositions obtained from these mixtures were as follows:

(1) $0.58\text{Al}_2\text{O}_3:\text{P}_2\text{O}_5:x\text{C}_{16}\text{TACl}:3.44\text{TMAOH}:348\text{H}_2\text{O}$, where $x=0.24-0.74$

(2) $1.16\text{Al}_2\text{O}_3:\text{P}_2\text{O}_5:x\text{C}_{16}\text{TACl}:1.80\text{TMAOH}:346\text{H}_2\text{O}$, where $x =0.24-0.74$

The synthesis mixtures were conducted at both 25 and 110°C and were otherwise treated in the same manner as in Section 3.2.

3.2.2.4 Effect of water concentration

Three various water concentrations on each of the two reaction mixtures of different Al/P

ratios (0.58 and 1.15) were conducted. For mixtures with Al/P ratio=0.58, the water weights were 28.8, 57.5 and 230 g while for mixtures with Al/P ratio=1.15, the weights used included 28.7, 57.5 and 230g. The mixtures were conducted at 25 and 110°C with the following molar compositions:

(1) $0.58\text{Al}_2\text{O}_3:\text{P}_2\text{O}_5:0.50\text{C}_{16}\text{TACl}:2.30\text{TMAOH}:w\text{H}_2\text{O}$, where $w= 86.0-689$

(2) $1.15\text{Al}_2\text{O}_3:\text{P}_2\text{O}_5:0.48\text{C}_{16}\text{TACl}:1.48\text{TMAOH}:w\text{H}_2\text{O}$, where $w= 86.0-687$

The mixtures were otherwise treated as in Section 3.2.

3.2.3 Synthesis of aluminophosphates using Psuedobohemite alumina

Pseudobohemite alumina was another choice of aluminum source that is widely used in the synthesis of microporous and mesoporous materials. We investigated the products that were obtained by using this aluminum source.

3.2.3.1 Effect of Al/P ratio

Four different synthesis mixtures were prepared, each containing 2.57, 3.42, 5.14 and 10.3g of pseudobohemite alumina, giving the following molar composition:

$x\text{Al}_2\text{O}_3:\text{P}_2\text{O}_5:0.50\text{CTACl}:2.98\text{TMAOH}:350.0\text{H}_2\text{O}$, where $x=0.59-2.34$. The mixtures were otherwise treated as in Section 3.2. 1.

3.2.3.2. Effect of water concentration

The water concentration was varied at each of the two reaction mixtures at different Al/P ratios (0.58 and 1.17) were conducted. The water weights at both ratios were 28.8, 57.5 and 230 g.

The molar composition for these synthesis mixtures were as follows:

(1) $0.86\text{Al}_2\text{O}_3:\text{P}_2\text{O}_5:0.50\text{C}_{16}\text{TACl}:3.22\text{TMAOH}:x\text{H}_2\text{O}$, where $x= 87-700$

(2) $0.43\text{Al}_2\text{O}_3:\text{P}_2\text{O}_5:0.50\text{C}_{16}\text{TACl}:3.26\text{TMAOH}:x\text{H}_2\text{O}$, where $x= 87-700$

The synthesis mixtures were otherwise treated as in Section 3.2.1.

3.2.3.3 Synthesis of cobalt and magnesium and organic containing aluminophosphates

In a typical synthesis, 4.74g CTAC, 10.79g TMAOH, 2.02mL H₃PO₄ and 8.75g distilled water were mixed for several hours, then 6.14g Al(OPr)₃ was added to the solution under vigorous stirring until the homogenous solution was obtained, pH value was adjust to 8.5 with TMAOH, organosiloxane was added to the mixtures. The mixture was stirred for 0.5h and dispersed in distilled water at 25°C. Organo-aluminophosphates were synthesized under otherwise similar conditions, but with the following organics added to the synthesis mixtures (1,2 bis-trimethoxysilylethane labeled as BTSE, 3-mercaptopropyltriethoxysilane, labeled as -SH, 3-aminopropyltriethoxysilane labelled -NH, and propyltriethoxysilane, labeled as Propyl) to be incorporated as part of the pore walls structure or be grafted by silane linkages. The typical molar ratio: 0.5Al₂O₃ : 1 P₂O₅ : 1CTAC : 2 TMAOH : 65 H₂O: 0.75 Si.

3.3 Calcination

The as-synthesized, dried samples were calcined in a Thermolyne tube furnace to remove the organic template. The samples were placed in a quartz boat, placed in the tube furnace, and heated to various temperatures slowly up to 500°C in the presence of flowing nitrogen, followed by oxygen at 70ml/min.

3.4 Characterization

3.4.1 X-ray powder diffraction

The crystallinity of the materials was characterized by the X-ray powder diffraction method using a Philips XPERT diffractometer with Cu-K_α radiation and nickel filters. The samples were first ground into fine powders and then packed into aluminum sample holders. The sample holder was mounted in the path of the x-ray beam and the instrument started by turning on the x-ray source through the computer interface. The X-ray source was a Cu-K_α anode, and the voltage and current were maintained at 40 KV and 50 mA, respectively. The diffractometer was programmed to scan diffraction angles from 2θ of 1 to 25° at a step size of 0.02 (2θ) and a step time of 10 second.

3.4.2 Surface area and pore size distribution analysis

Multiple point BET surface area and pore size analysis was done on the calcined products using a Micromeritics Gemini 2360 Surface Area Analyzer and a Micromeritics ASAP2020 porosimeter. To determine surface area and pore size measurements, a preweighed portion of

each sample was placed in a tube and degassed for 2 hr at 200°C to remove adsorbed contaminants acquired from atmospheric exposure. The sample was placed in the BET analyzer and adsorption was performed at 77 K using nitrogen as an adsorbate. Relative pressure range (P/P_0) of 0.1-0.3 and 0.1-1.0 P/P_0 was used for surface area and pore size analysis respectively. The Barret, Joyner and Halenda (BJH) model was used to calculate the pore size distribution from the relative pressure and volume obtained from BET data.

3.4.3 Thermogravimetric analysis

TGA analysis was performed on a SDT 2960 TA instruments Inc. Milligram quantities of each sample was placed in a ceramic crucible. The sample was heated at an ambient to 700°C at a heating rate of 10°/min in flowing air.

3.4.4 Solid State Magic Angle Spinning NMR analysis

²⁷Al MAS NMR measurement was performed on a DSX-400 spectrometer at a resonance frequency of 104.181-MHz, spinning rate of 7.5 KHz with a 45° pulse length of 4.5psec. For each spectrum, 128 scans was acquired with a 5 sec repetition between scan. Aluminum nitrate was used as external reference. ³¹P MAS NMR spectra were measured at a resonance frequency of 161.86 MHz with 60° pulse length of 5.0 sec at a spinning rate of 9.9 KHz, 32 scans and a 30s repetition between scans. ³¹P chemical shifts were quoted with respect to external 85%, phosphoric acid.

3.4.5 Chemical analysis

The aluminum and phosphorus compositions of samples were determined by ICPMS using the Perkin Elmer Elan 5000 instrument. The samples were prepared by mixing accurately weighed aliquots (6mg) of sample with 25 mg of sodium borate ($\text{Na}_2\text{B}_4\text{O}_7 \cdot 10\text{H}_2\text{O}$). The mixtures were fused (melted) in a platinum crucible at 700°C in a Fisher Scientific Isotemp muffle furnace. After 21 hr the melt was allowed to cool slowly. The solid mass was then dissolved in 5ml of hot concentrated HNO_3 acid, placed in a 100ml volumetric flask and made up to the mark with deionized water. The solution was then diluted by a 100 fold with deionized water and ICP-MS analysis was performed. Standard solutions for analysis of Al and P was prepared by taking appropriate amounts of certified stock standard (10 µg/ml of P and 100 µg/ml of Al, Accustandard Co) into a 100 ml volumetric flask and filled to the mark with 1 % HNO_3 acid. From this solution the following working standards were prepared:

10ppb, 50ppb, 100ppb, 500 ppb and 1000 ppb.

3.4.6. Infrared Spectrometry

Infrared spectroscopy analysis was performed with a Hai'lick high- -vacuum temperature-controlled stainless steel reaction chamber (HVC) diffuse reflectance accessory fitted to a Nicolet 750 Magna IR. Sample preparation was obtained by mixing, milligram quantities of finely ground sample with approximately 5mg of the KBr powder. This was then placed in a cell and analyzed.

3.4.7 Catalytic Testing

A single pass fixed bed continuous flow reactor catalytic reactor interfaced with a Gas Chromatograph was set up for evaluating cumene cracking (Scheme 1). The instrument is currently undergoing calibration prior to catalyst evaluation. For cumene cracking, a nitrogen stream will be saturated with cumene which is placed in a saturator, and subsequently carried at various space velocities over a catalyst bed (~0.5 gm) in a tube reactor which will be heated at a predetermined temperature and space velocity. The catalytic products will be sampled on-line using a 6 port sampling valve and injected onto the GC for analysis. Product distribution will be assessed for zeolite Y/Nnaocomposite host of various physicochemical characteristics.



Scheme 2. Pictorial of the reactor used for catalysis

4.0 RESULTS AND DISCUSSION

4.1 Synthesis of mesostructured aluminophosphate with aluminum hydroxide

The composition of the starting mixtures for various Al/P ratios was as follows: $x\text{Al}_2\text{O}_3:\text{P}_2\text{O}_5:0.5\text{C}_{16}\text{TAC}1:2.6\text{TMAOH}:351\text{H}_2\text{O}$, where x was varied from 0.3 to 2.3. Depending on the Al/P ratios of the synthesis mixtures, X-ray diffraction patterns in Figure 1 indicate that a lamellar and or hexagonal phase was obtained. For samples with Al/P ratio 0.33-1.25, the XRD patterns show a prominent peak at 2θ of 2.1° , corresponding to the hkl [100] lattice reflections with a d-spacing of 4.0 nm and a much weaker, but clearly present peak at 2θ of 3.8° corresponding to hkl (110) reflections. This combination of peaks are reported to correspond to a hexagonal lattice. For sample with Al/P ratio= 0.29, the XRD pattern show a main peak at 2θ of 2.1° corresponding to d-spacing of 3.1 nm, and a second peak at 2θ of 5.1° corresponding to d spacing of 3.51nm and several peaks in the 2θ region including a peak higher than 15° . This combination of peaks are characteristic of a lamellar phase.¹⁴

The ^{27}Al and ^{31}P MAS NMR spectra of the lamellar and hexagonal phases prepared from reaction mixture with Al/P=0.58 are shown in Figure 2. The NMR spectrum of lamellar phase showed a sharp signal at 42.5 ppm indicating the presence of four-coordinated Al, which can be assigned to Al (OP)₄ units. A small peak observed at -5.1 ppm is assigned to small amounts of six-coordinated Al.⁷ The ^{31}P MAS NMR spectrum for the lamellar phase shows two peaks at -19.1 and -22.6 ppm, both of which are assignable to OP(OAl)₃ units.⁷

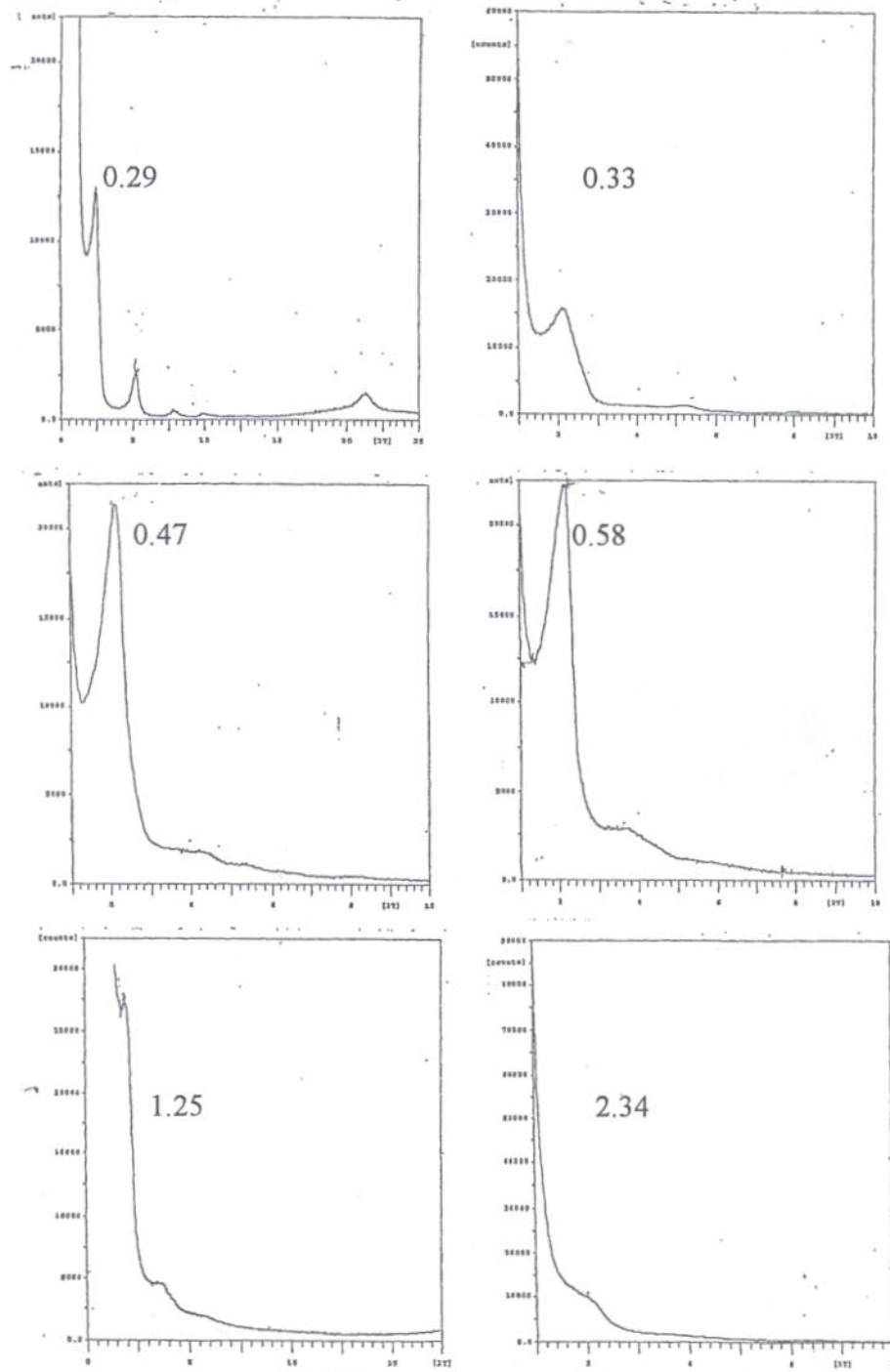


Figure 1: XRD patterns of samples at various Al/P ratios in synthesis mixture

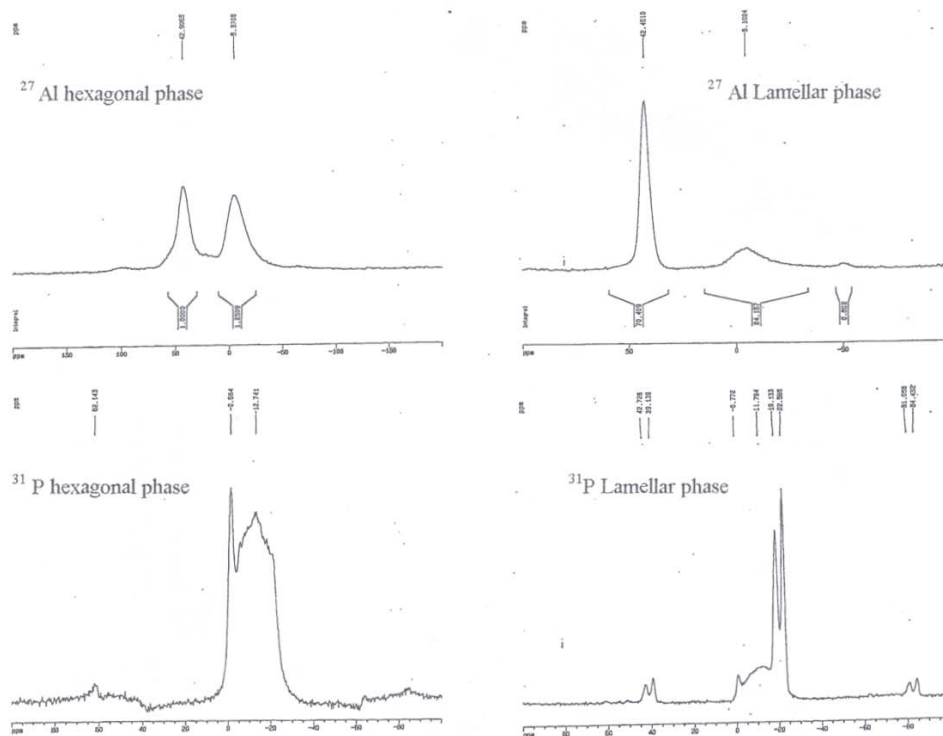


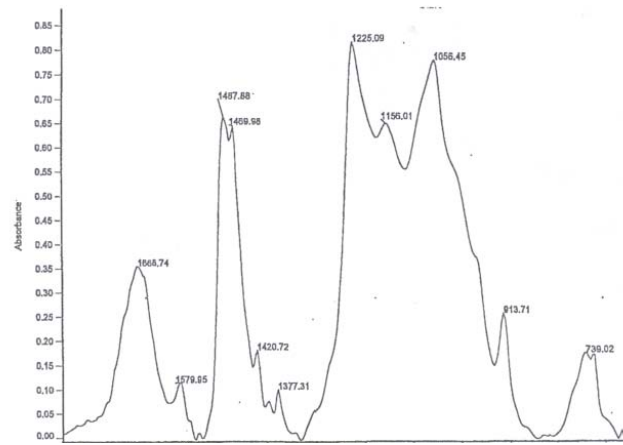
Figure 2: ^{27}Al and ^{31}P SS MAS NMR of lamellar and hexagonal phases at 0.58 Al/P ratio (25°C)

The ^{27}Al MAS NMR spectra for the hexagonal phase indicate two different chemical shifts. The signal at 42.9 ppm is assigned to four-coordinated Al bonded to phosphorus atoms via oxygen bridges to form AlPO_4 and or $\text{Al}(\text{OP})_{4-x}(\text{OH})_x$. The peak at - 5.4 ppm is attributed to the framework octahedral aluminum, coordinated possibly with both water and PO_4 groups. The ^{31}P MAS NMR spectrum for hexagonal phase shows several peaks ranging from 0 to -20 ppm. Two peaks at -12.7 and - 4.95 ppm were observed. Mortlock *et.al* reported that the P atoms in $\text{Al}(\text{H}_2\text{O})_5(\text{H}_3\text{PO}_4)$, $\text{Al}(\text{H}_2\text{O})_4(\text{H}_3\text{PO}_4)_2$ and $\text{Al}(\text{H}_2\text{O})_4(\text{H}_3\text{PO}_4)(\text{H}_3\text{PO}_4)$ are observed at -12.6 ppm and $-\text{P}(\text{OAl})_4$ units are observed at -

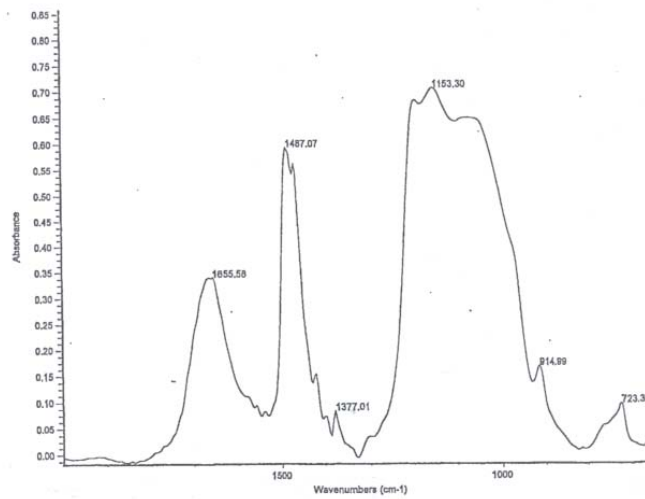
0.98.¹⁶ Phosphorous present in hexagonal phase in Figure 2 may therefore be attributed to tetrahedral phosphorus bonded to aluminum tetrahedra and hydroxyl groups or water. The reported chemical shifts of ³¹P in microporous AlPO₄- type materials generally fall in the range -19 to -30 ppm.⁷ The shift of the ³¹P NMR signal to lower fields can be caused by several factors; monovalent cations, acid protons, and coordinated water can all cause downward shifts in the spectra of phosphates.⁷ PO₄ units are therefore bonded to one or two Al atoms, suggesting the hexagonal phase has a less condensed framework.¹⁴

The IR spectrum of the lamellar and hexagonal phases described above, are shown in **Figure 3**. The lamellar phase shows several peaks in the region of 1668 - 739 cm⁻¹. The region of 1225-1056 cm⁻¹ and 739 cm⁻¹ are due to the asymmetric stretching of Al-O-P and the symmetric stretching of Al-O-P respectively. The hexagonal phase shows several peaks in the 1655 to 723 cm⁻¹ region. The peaks at 1487 cm⁻¹ and a broad peak at 1153 cm⁻¹ correspond to the asymmetric stretching of Al-O-P and the peak located at 723 cm⁻¹ is due to the symmetric stretching of Al-O-P.¹⁴ IR analysis therefore provided further evidence for the presence of Al-O-P bonding in the products.

Figure 4 shows the thermograms obtained from the thermogravimetric analysis of the lamellar phase from samples synthesized with Al/P=0.29 in mixture, and hexagonal phase from samples with Al/P=0.58. A total weight loss of 67.3% for lamellar phase and 60.03 % for hexagonal phase is exhibited in three stages. The weight loss events at 80°C, 121°C and 353°C for both lamellar and hexagonal phase correspond to water desorption and decomposition of CTACl and TMAOH respectively. For samples with Al/P ratio= 0.29, a 52% weight loss corresponding to the loss of the CTACl was obtained while at Al/P ratio = 0.58 a 41% weight loss was determined. TGA analysis also established that heating of the samples could be conducted at < 400°C to remove the organics.



A) Lamellar phase



B) Hexagonal phase

Figure 3: IR Spectrum of A) Lamellar B) Hexagonal Phase

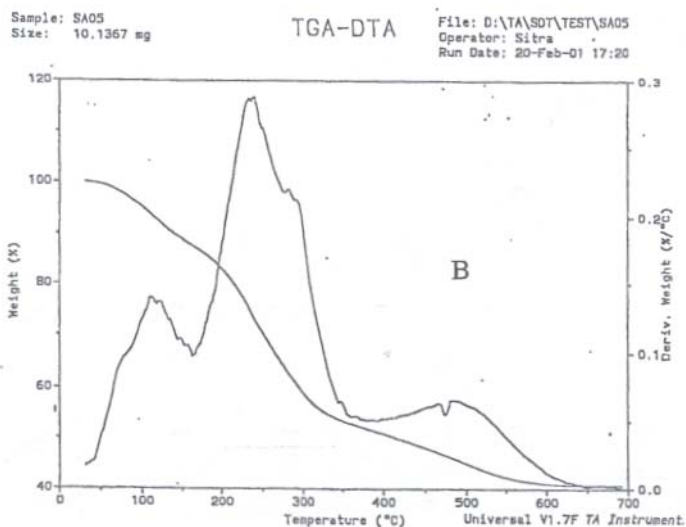
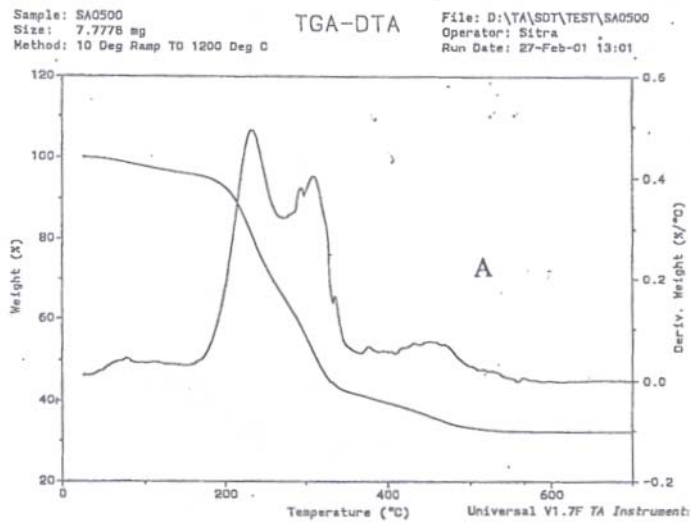


Figure 4: TGA/DTA data of A) Lamellar and B) Hexagonal phase

4.1.1 Effect of Al/P ratio

For sample synthesized with Al/P ratio < 0.33 in mixture, a lamellar phase was observed in the diffractogram with major peak at 2θ of 2.7° corresponding to $d(100)$ spacing of 3.5nm shown in Figure 5. As the synthesis Al/P ratio increased to the range 0.33-1.25 the hexagonal phase

was obtained, with a main peak at 2θ of 2.1° corresponding to a d (100) spacing of 4.1 nm and a smaller peak at 2θ of 3.9° with a d (110) spacing of 1.4 nm. For the hexagonal phase, peaks were most defined within Al/P ratios of 0.47-1.25. Highest lattice ordering were therefore obtained in this range. At higher Al/P ratio (>1.25), a broad, low intensity peak was observed due to a disordered hexagonal array. Aluminophosphates can form over a range of Al/P mole ratios (0.29-2.34) in the gel, which is different from a fixed Al/P ratio required for synthesis of microporous aluminophosphates.

The Al/P ratio in the product as indicated in Table 1 increases with increasing Al/P ratios in the gel. The Al/P ratio less than 1.25 in the mixture show better resolved XRD patterns. This is because the Al/P ratios in the products range from 1.64-0.92 which correspond to the ideal $\text{Al}(\text{PO})_4$ coordination. This was also observed by Kimuru et al who reported that Al/P ratios of the products increased with increase in Al/P and TMAO/P ratio in the synthesis mixture. This is perhaps why the products showed better resolved XRD patterns with Al/P ratio <1.25 .

Table 1 : Effect of Al/P composition of starting mixtures on Al/P ratio in products

Al/P ratio	pH of mixture	Al/P ratio of products obtained
0.29	7.31	0.92
0.33	7.37	1.01
0.47	8.01	1.53
0.58	8.46	1.64
1.25	9.42	2.45
2.34	9.50	5.31

(* RPD= Relative percent difference from 2 determinations $2(A-B)/(A+B)$)

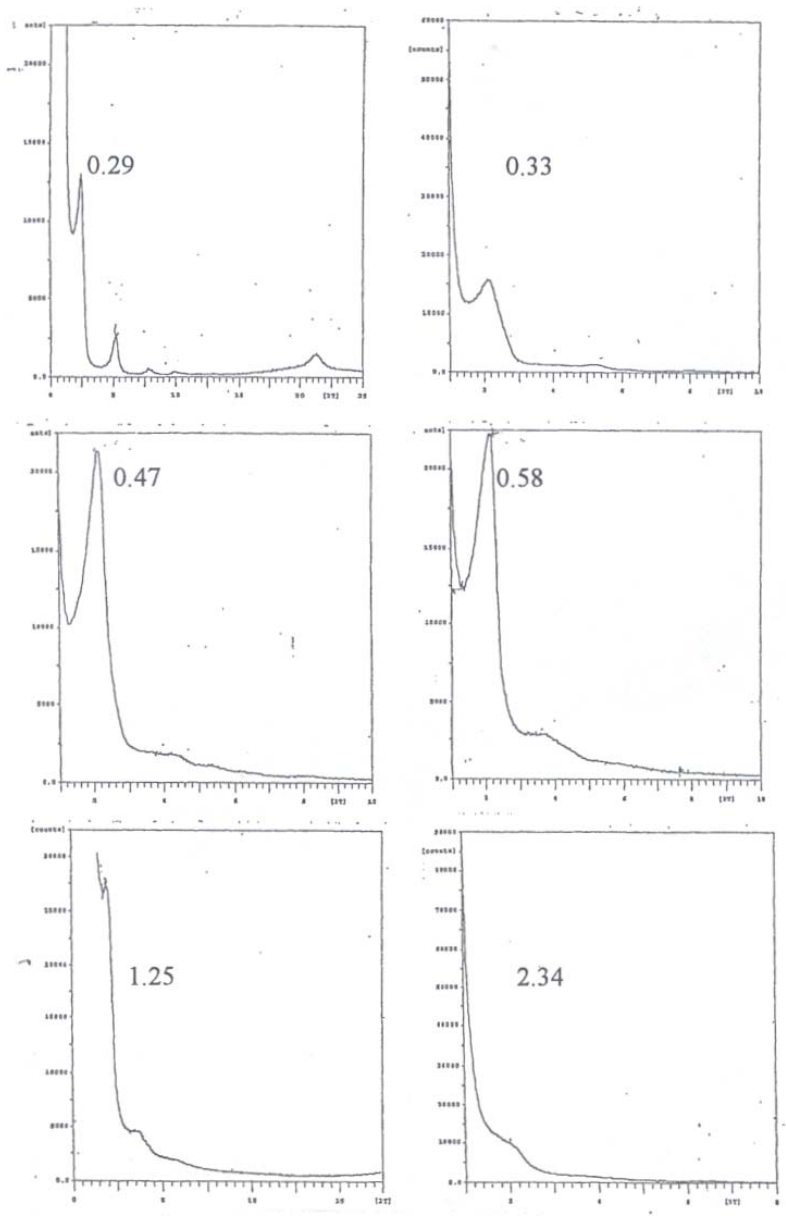


Figure 5: XRD patterns at various Al/P ratios

In order to determine the thermal stability of the as synthesized materials, calcination at 500°C for 1 hour in nitrogen followed by air was conducted to remove the occluded organic template. Amorphous products were obtained for all Al/P ratios except for Al/P of 1.25 (**Figure 6**). At this ratio X-ray patterns indicated a partial loss in intensity of the main peak at 2θ of 2.1° , from

28000 counts in the as-synthesized material to 15000 counts in the calcined form. Peak broadening was also observed. Surface area of the calcined product was 446 m²/g. This observation is likely due to the loss of crystallinity of the hexagonal array when subjected to calcination. In order to examine the temperature at which the mesoporous materials lost stability, calcinations as low as 300°C under flowing N₂ for 1 hour was conducted. This also resulted in a structural collapse, as evidenced by loss of peaks in X-ray diffraction patterns and extremely low BET surface areas. An alternative organic extraction to remove the template using sodium acetate/ethanol mixture also resulted in similar structural collapse.

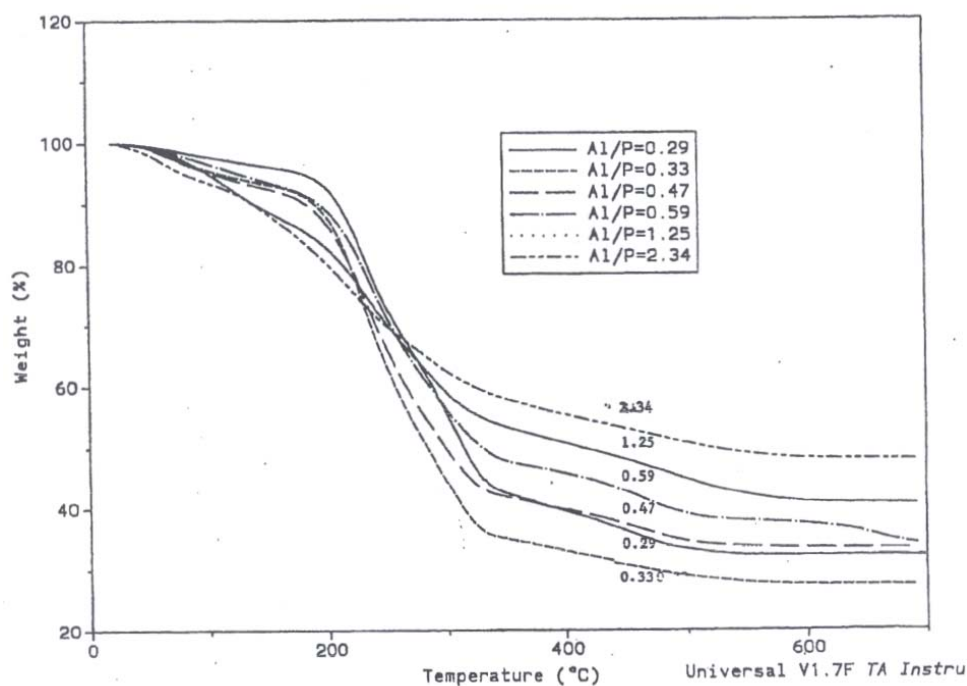


Figure 5B. Thermograms of mesoporous aluminophosphates synthesized under various Al/P ratio.

Table 2. Weight loss events from TGA Analysis of mesoporous aluminophosphates

Al/P = 0.29		Al/P = 0.33		Al/P = 0.47		Al/P = 0.58		Al/P = 1.25		Al/P = 2.34	
Temp (C)	Wt Loss	Temp (C)	Wt. Loss	Temp (C)	Wt. Loss	Temp (C)	Wt Loss	Temp (C)	Wt. Loss	Temp (C)	Wt. Loss
25 - 186	5.5	53-187	8.6	54-190	10	66-201	9.8	97	15	53	6.1
186 -353	52	187-338	55	190-337	46	201-351	41	210-336	27	122-341	33
353 -500	9.8	338-500	3.6	337-500	4.6	351-500	9.2	336	13	341	17
Total Wt Loss (%)	68		67		61		60		54		56

The development of porosity in the products can be inferred from desorption of occluded species using thermogravimetric analysis. Figure 5b shows thermograms of products obtained at various Al/P ratios. The corresponding weight loss events for these products are presented in Table 1. Desorption events in the regions of 200°C, 350°C, and 500°C for sample with Al/P ratio of 0.59 for example, are ascribed to water loss, decomposition of CTA⁺, and TMA⁺ organic species respectively. Samples with Al/P ratio 2 to 1.25 showed relatively small loss of organic species, compared with samples synthesized at lower Al/P ratios. Lower Al/P ratio samples showed desorption of CTA⁺ corresponding to approximately 40-55 % of sample wt.

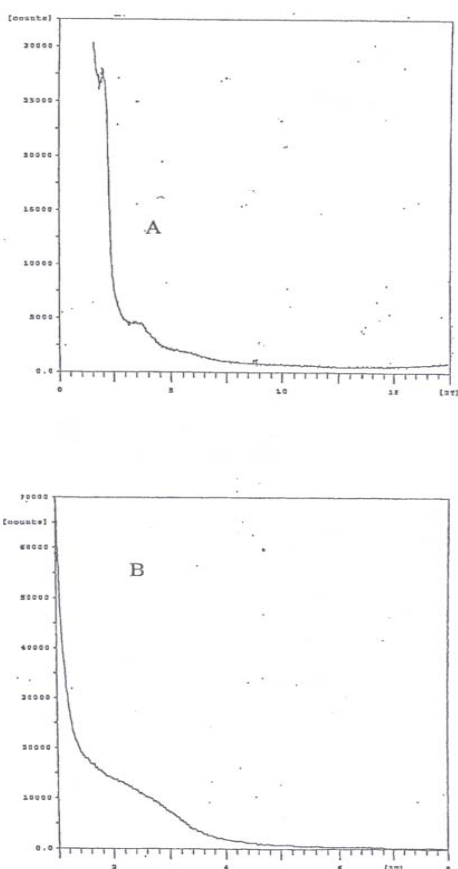


Figure 6: XRD data of a) as-synthesized, and b) calcined Al/P ratio at 1.25

Since the mesoporous materials formed above indicated low thermal stability it was considered that an increase in pore wall thickness might result in a stabilized framework upon calcination. Therefore, the effects of several reaction parameters on the synthesis and thermal stability of mesoporous aluminophosphates were investigated. Among these parameters were: TMAOH and surfactant concentration, the aluminum source as well as reaction temperature and time.

4.1.2 Effect of TMAOH concentration

The TMAOH content of the starting mixtures were changed for three different Al/P ratio as follows:

- (1) $0.58\text{Al}_2\text{O}_3:\text{P}_2\text{O}_5:0.50\text{C}_{16}\text{TMACl}:x\text{TMAOH}:347\text{H}_2\text{O}$, $x = 1.06\text{-}3.64$
- (2) $1.17\text{Al}_2\text{O}_3:\text{P}_2\text{O}_5:0.50\text{C}_{16}\text{TMACl}:y\text{TMAOH}:344\text{H}_2\text{O}$, $y = 0.78\text{-}3.36$
- (3) $1.77\text{Al}_2\text{O}_3:\text{P}_2\text{O}_5:0.50\text{C}_{16}\text{TMACl}:z\text{TMAOH}:350\text{H}_2\text{O}$, $z = 0.68\text{-}2.80$

The XRD patterns of the products obtained from molar composition (1) above and synthesized at room temperature is shown in **Figure 7**. In the absence of TMAOH or with TMA/P₂O₅ ratio up to 1.06 (pH 5.2) amorphous products were observed. With further increase in the amount of TMAOH, the structure of the products changed from lamellar to hexagonal. At TMA/P₂O₅ of 1.48 (pH 6.51) a combination of hexagonal and lamellar type products with major peaks at 2θ values of 2.6 and d spacing of 3.33nm were observed respectively.

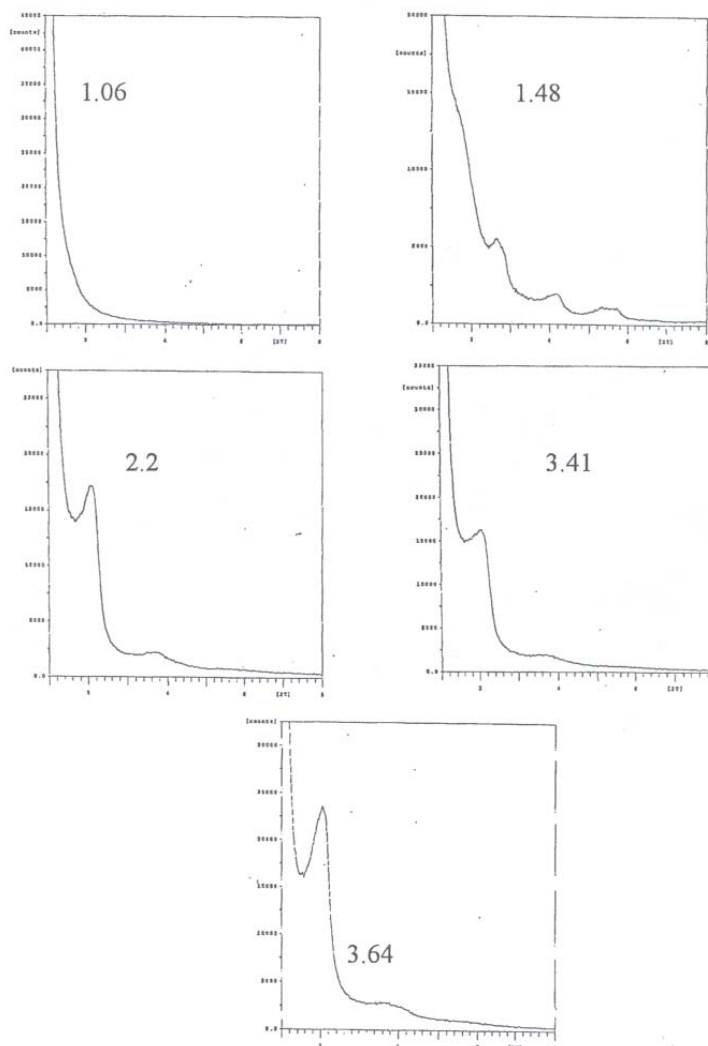
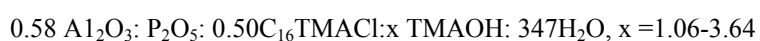


Figure 7: Effect of TMAOH concentration at 0.58 Al/P, 25°C



Increase in the TMA/P₂O₅ ratio 2.2-3.64 (pH 8.0-10.4) resulted in the hexagonal phase as the only ordered phase. Conducting the synthesis at 110°C (**Figure 8**) gave lamellar phase for TMA/P₂O₅ ratio as high as 2.2 (pH 7.95). At this temperature, hexagonal phase formed at much higher TMA/P₂O₅ ratios of 3.44 and 3.64. A combination of low Al/P ratio and high TMA⁺ therefore favors the formation of hexagonal phase at room temperature and lamellar phase at high temperature.

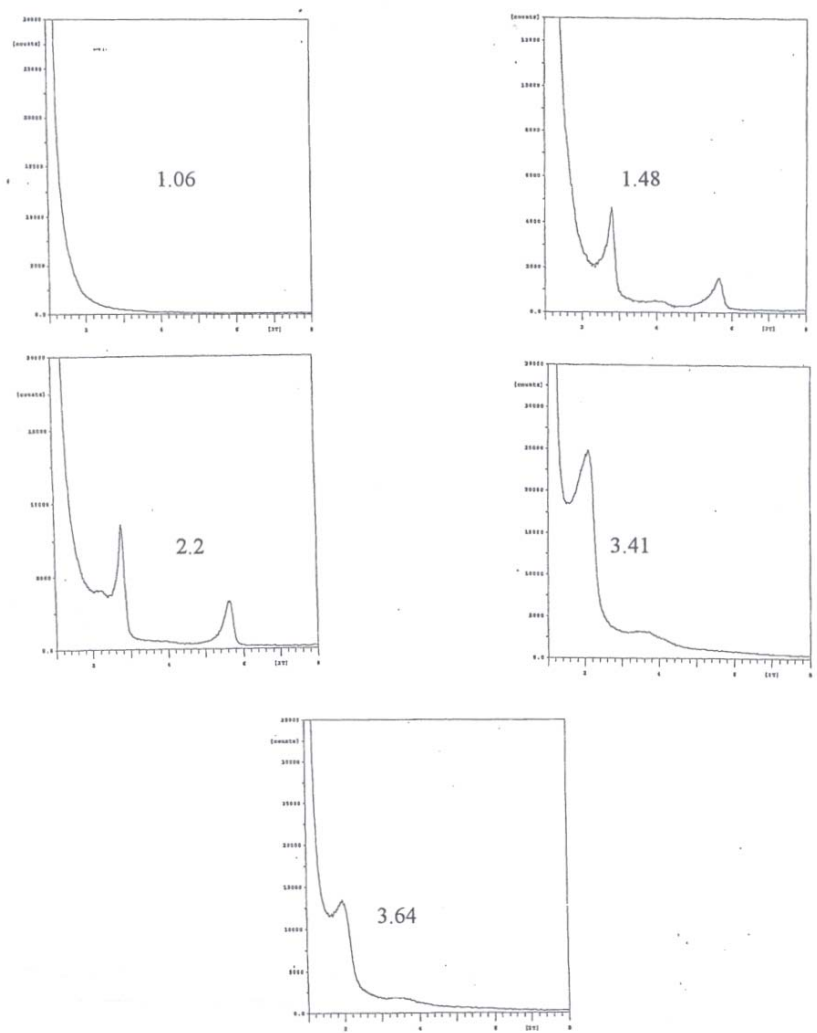


Figure 8: Effect of TMAOH concentration at Al/P = 0.58, 110°C
 0.58 Al₂O₃: P₂O₅:0.50C₁₆TMAC1:xTMAOH: 347H₂O, x =1.06-3.64

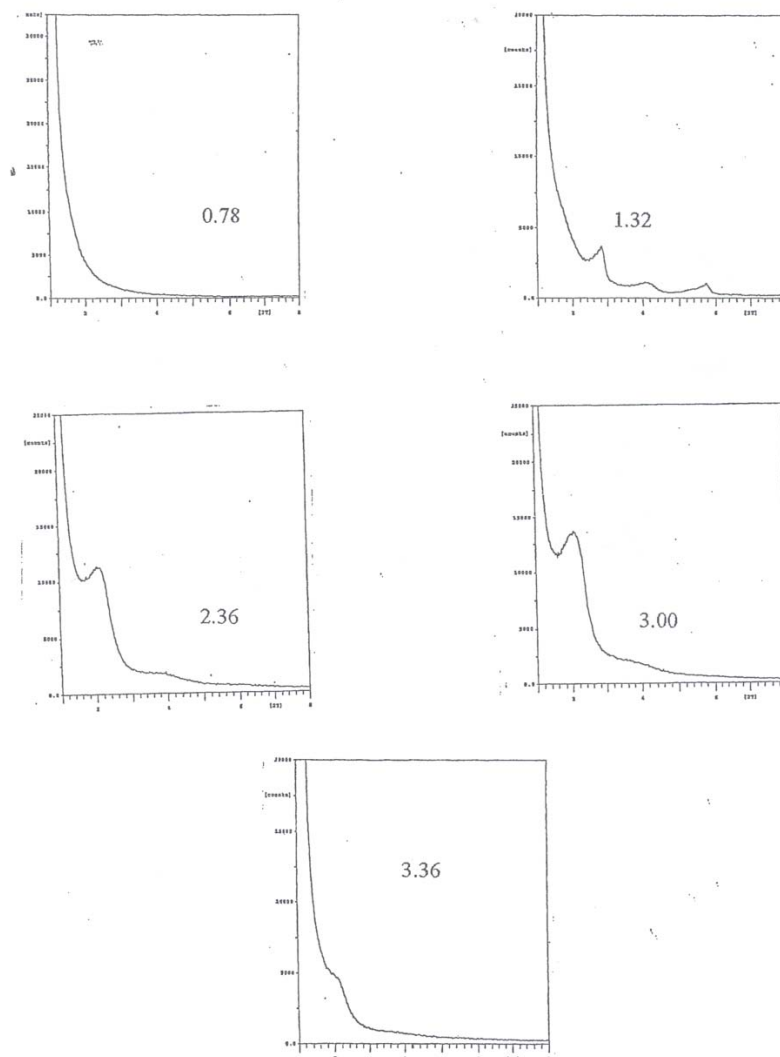


Figure 9: XRD patterns of products obtained from synthesis mixtures of various TMAOH/P₂O₅ ratios and fixed Al/P of 1.17 (synthesis conducted at 25°C) (TMAOH/P₂O₅ ratios indicated on graph)

The formation of the mesoporous aluminophosphate materials is postulated to occur by a modified S⁺I ion-pair process.¹³ It is reported that the inorganic precursors (IP) are nonideal aluminophosphate species of low polymerization degree with some hydroxyl groups. When tetramethylanunonium hydroxide is added, it reacts with the hydroxyl groups of these aluminophosphate species to produce a weak ion pair (I...TMA⁺) since the TMA⁺ cation has a large ionic radius. These ion-pair species diffuse to the surfactant (S') assembly (micelle) interface and interact strongly with the cationic surfactant headgroups. The interaction of the aluminophosphate species with the cationic surfactant headgroups is stronger than that with TMA⁺ cation. The micellar structure then organizes the condensation and polymerization of adjacent aluminophosphate species to form an ordered hexagonal mesostructure.¹³

The function of the organic ammonium cation from TMAOH therefore, seems to be to modify the strength of the electrostatic interaction between the aluminophosphate species and the cationic surfactant micelle assembly to form S⁺ L... TMA⁺ ion pair. It is reported that if NaOH is used instead, the Na⁺ cation has a smaller ionic radius than TMA⁺ cation, which possesses a stronger ion-pair interaction with the aluminophosphate species and therefore prevents sufficient interaction with the cationic surfactant assembly. Thus the assembly of mesostructural aluminophosphate fails.¹³

In addition, TMA⁺ also affects the phase change as indicated in Figure 4. The TMA⁺ concentration suppresses the polymerization of the aluminophosphate oligomers resulting in incomplete condensation occurring in the hexagonal phase as observed earlier by NMR data.¹⁴ On the other hand, lamellar phase has a regularity of Al-O-P- bonds, which affords a relatively condensed framework. Furthermore, the hydroxide species from TMAOH facilitates the hydrolysis of the inorganic precursors, so an increase in TMAOH concentration also resulted in more species that are hydrolyzed. With an increase in the synthesis temperature to 110°C, the progress of the condensation of inorganic species led to the formation of lamellar phase.

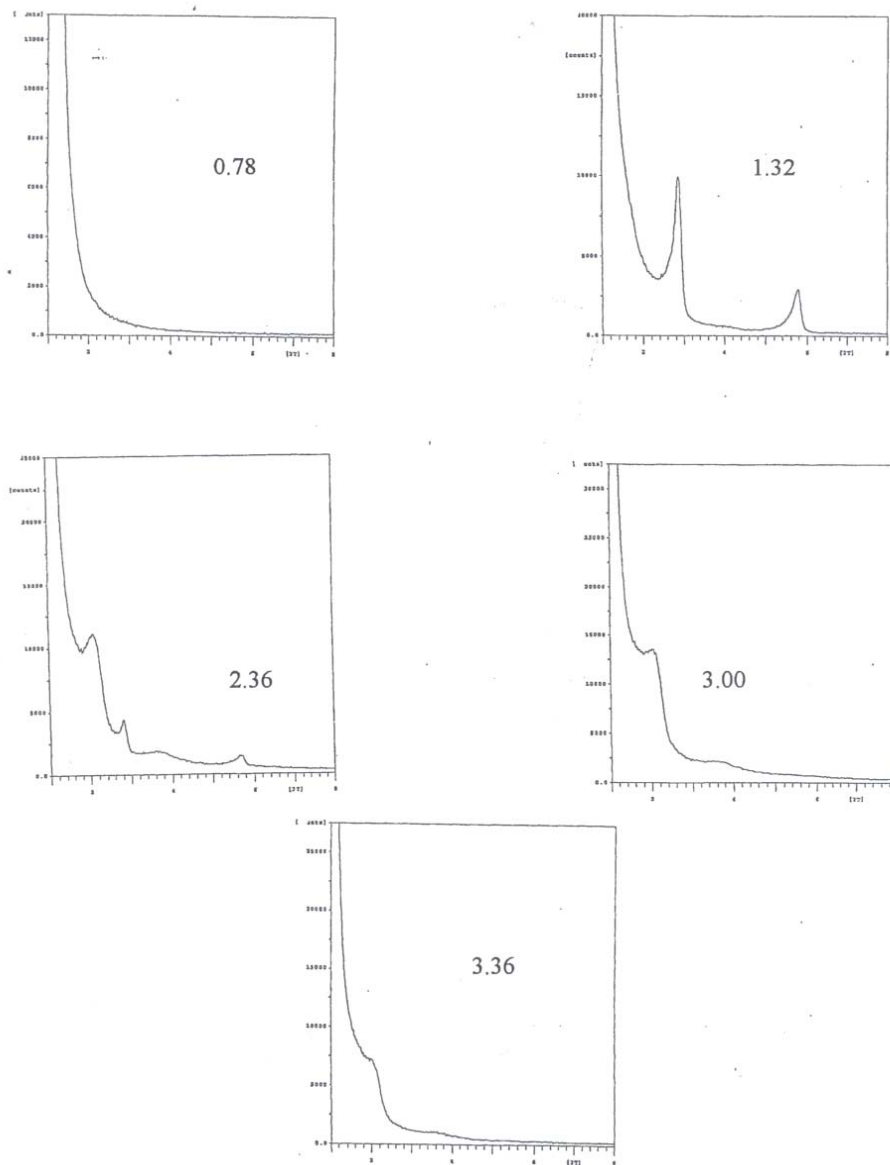


Figure 10: XRD patterns of products obtained from synthesis mixtures of various TMA/P₂O₅ ratios and fixed A/P of 1.17 (synthesis conducted at 25°C) (TMA/P₂O₅ ratios indicated on graph)

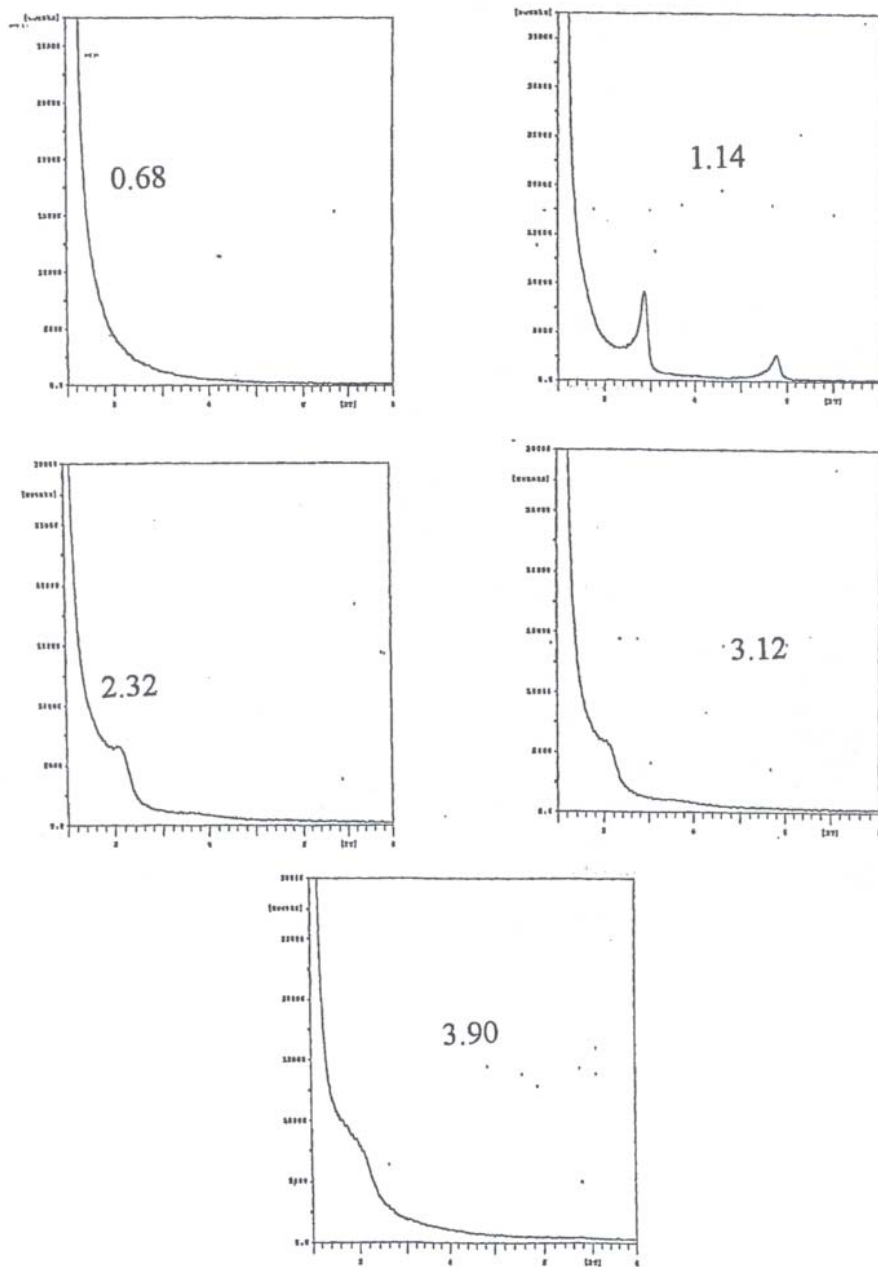


Figure 11: XRD patterns of products obtained from synthesis mixtures of various TMA/P₂O₅ ratios and fixed Al/P of 1.77 (synthesis conducted at 110°C) (TMA/P₂O₅) ratios indicated on graph)

XRD patterns from the synthesis mixture at Al/P ratio= 1.17 are shown in Figures 10 and 11 for synthesis conducted at 25°C and 110°C respectively. A similar trend is observed in Figure 7, except that a less ordered hexagonal phase was obtained at high TMA/P₂O₅ ratio of 3.64 (pH 10.03). Mokaya *et.al* reported that Al buried deep within the pore walls is known to reduce the structural ordering of aluminosilicate MCM-41, and may have a negative effect on stabilization of the framework.¹⁷ The position occupied by the directly incorporated Al may therefore be an important factor with respect to framework stabilization. Low Al contents may therefore favor the presence of Al predominantly on or near the surface, while in higher Al content materials the Al may occupy positions deeper within the pore walls. With the higher Al/P ratio synthesis (1.77) (Figure 11), the hexagonal product formed at the TMA/P₂O₅ ratio of 2.32 and room temperature decreased in quality. This may probably be due to the presence of high aluminum species that resulted in poor condensation. At higher temperature and Al/P ratio 1.77 (Figure 12), a hexagonal phase was initiated at lower TMA/P₂O₅ ratio of 2.32. As indicated above, high temperature, low TMA concentration and low Al/P ratio favors lamellar phase; but an increase in aluminum content may assist the formation of hexagonal phase at low TMA content. This may be due to a large amount of poorly condensed aluminum species that may override the effect of low TMA content.

The extent of the condensation of inorganic species is important in for the formation of both phases. Thus, it is necessary for the synthesis temperature to be lower in the preparation of the hexagonal phase in order to suppress the formation of condensed inorganic inorganic phases.

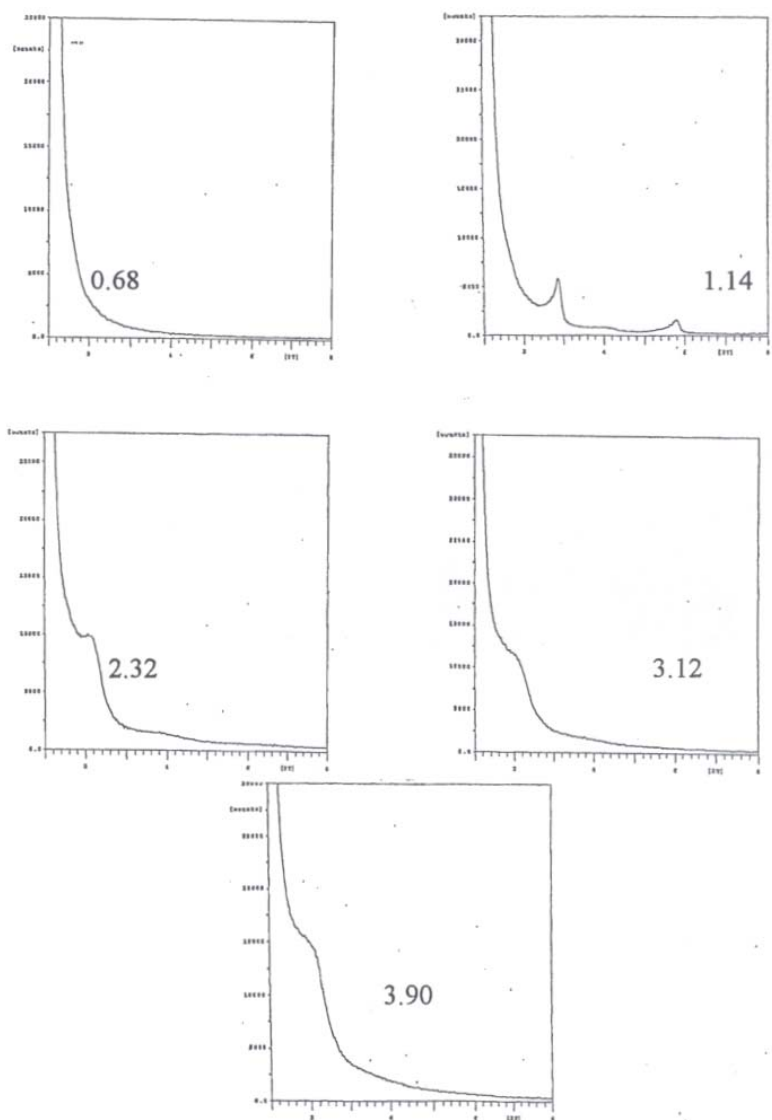


Figure 12: XRD patterns of products obtained from synthesis mixtures of various TMA/P₂O₅ ratios and fixed Al/P of 1.77 (synthesis conducted at 110°C) (TMA/P₂O₅ ratios indicated on graph)

4.1.3 Effect of surfactant concentration

Using the following molar composition, $0.58\text{Al}_2\text{O}_3\text{P}_2\text{O}_5\text{yC}_{16}\text{TACl}$: 3.44TMAOH : $348\text{H}_2\text{O}$, a series of samples were prepared where $y = 0.24-0.98$. The critical micellar concentration of CTACl in the aqueous medium is 1.30×10^{-3} M, the lowest CTACl concentration used in this experiment was 9.23×10^{-1} M. Thus the surfactant is expected to be in the micellar form. X-ray diffraction patterns in Figures 13 and 14 show that significant increase in crystallinity was observed as CTACl/ P_2O_5 was increased from 0.24 to 0.98. At CTACl/ P_2O_5 ratio of 0.98 a lamellar phase was observed at 25 and 110°C whereas crystalline hexagonal type structure was obtained between 0.24-0.72 CTACl/ P_2O_5 ratios. The fact that aluminophosphates can be synthesized from solutions containing only CTACl/OH micelles, suggests that the inorganic precursors form electrostatic bonding with surfactant cations. Once the inorganic precursor and the micelles are in place, the interfacial charge redistributes leading to the formation of mesophase with lower curvature. It can also be suggested that high CTACl facilitates more condensation, resulting in a lamellar phase.

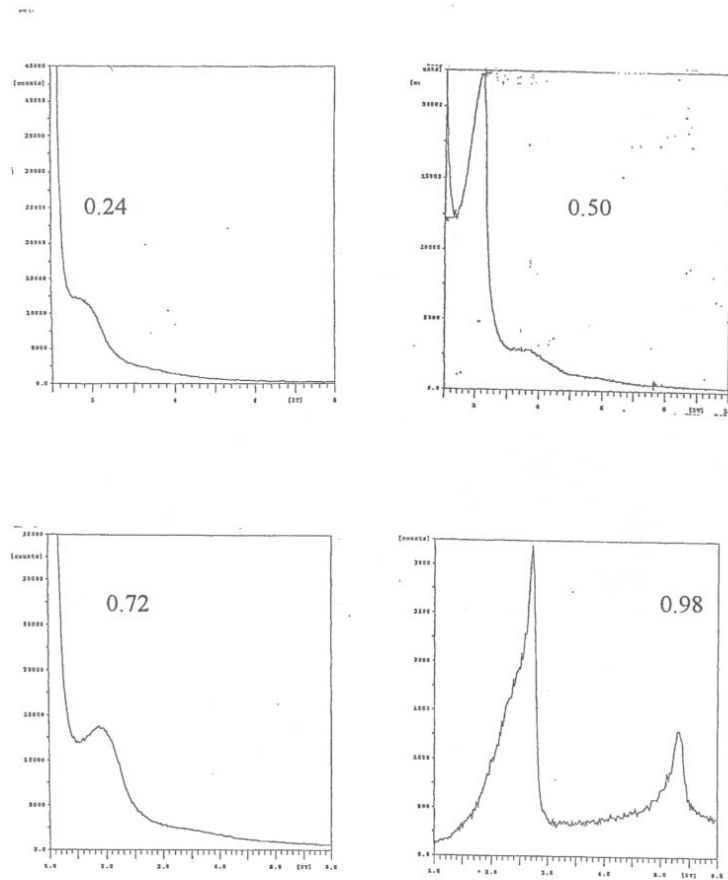


Figure 13: Effect of surfactant concentration at 0.58 A1/P, 25°C 0.58A1₂O₃:
P₂O₅: y C₁₆TAC1: 3.44TMAOH: 348 H₂O, y= 0.24-0.98

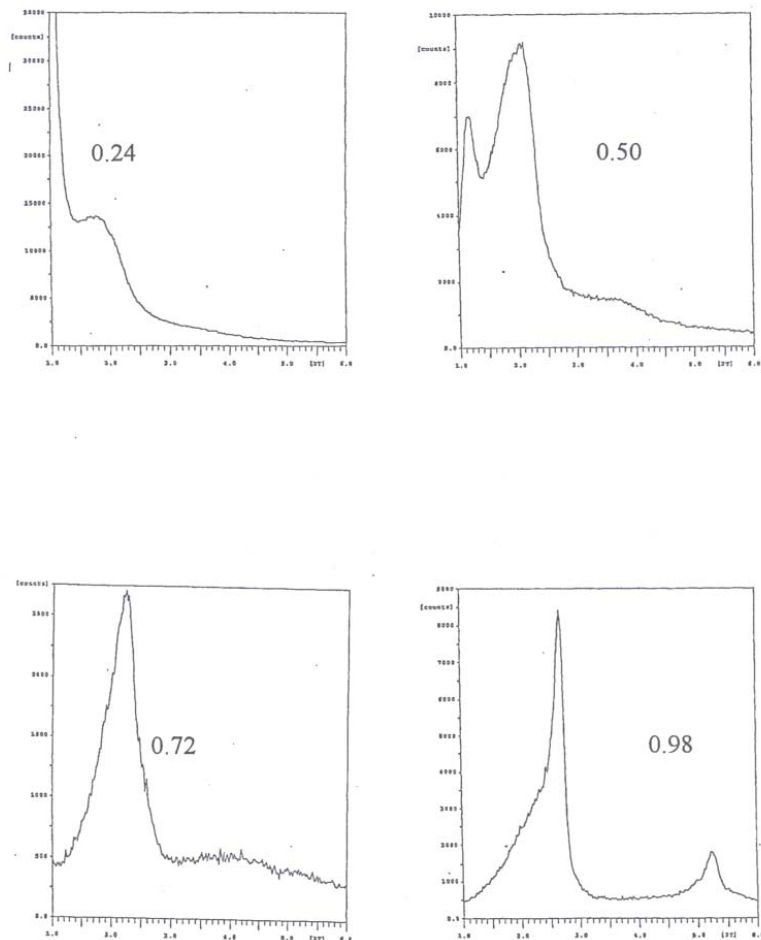


Figure 14: Effect of surfactant concentration at 0.58 Al/P, 110°C
 $0.58\text{Al}_2\text{O}_3 : \text{P}_2\text{O}_5 : y\text{C}_{16}\text{TACl} : 3.44\text{TMAOH} : 348 \text{H}_2\text{O}$, $y = 0.24\text{-}0.98$

4.1.4 Effect of synthesis time

Reaction mixture with molar composition $0.58\text{Al}_2\text{O}_3 : \text{P}_2\text{O}_5 : 0.50\text{C}_{16}\text{TACl} : 0.22\text{TMAOH} : 350\text{H}_2\text{O}$ was used to study the formation of mesoporous materials at 5, 10, 24, 48 and 72 hour period. Intermediate solid products collected in the course of the reaction were investigated. The degree of their crystallinity represented as the intensity of (100) XRD reflections, increases during the course of the reaction. A 0.5 and 2 hr mixing of aluminum and phosphorous prior to the addition of TMAOH was also carried out during the synthesis. For samples obtained from 0.5 hour mixing before TMAOH addition, X-ray diffraction (**Figure 15**) indicates hexagonal phase for all reaction times investigated and a solid product

were obtained even at 5 hrs. However, with 2 hrs mixing before TMAOH addition X-ray diffraction data in **(Figure 16)** indicated a highly disordered phase at 5hrs synthesis. The degree of crystallinity for 2hrs mixing time, represented as the intensity of X-ray diffraction reflections, increases from 10 to 72 hrs during the course of the reaction. This suggested that 24 hrs is adequate for mesoporous material synthesis.

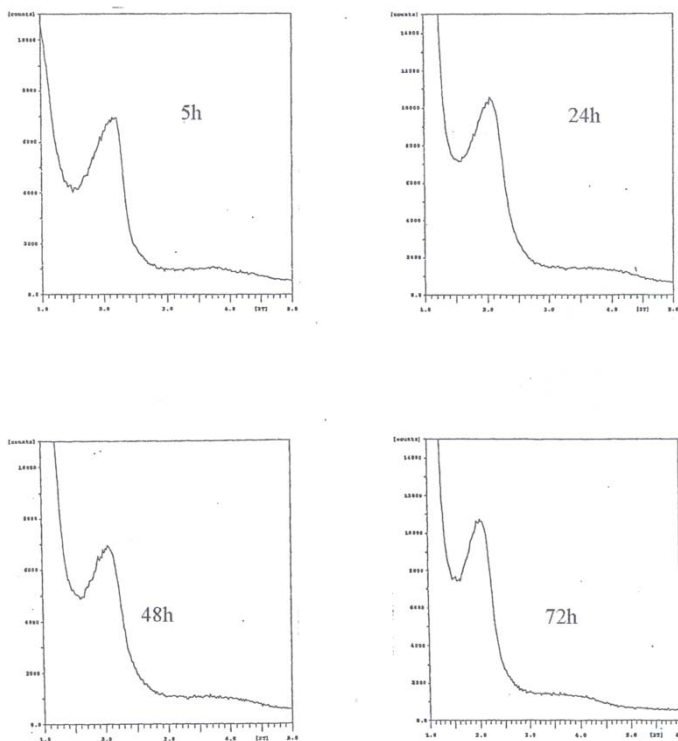


Figure 15: XRD patterns obtained for samples synthesized at various reaction times and fixed Al/P of 0.58 (0.5 hrs mixing before TM AOH addition)

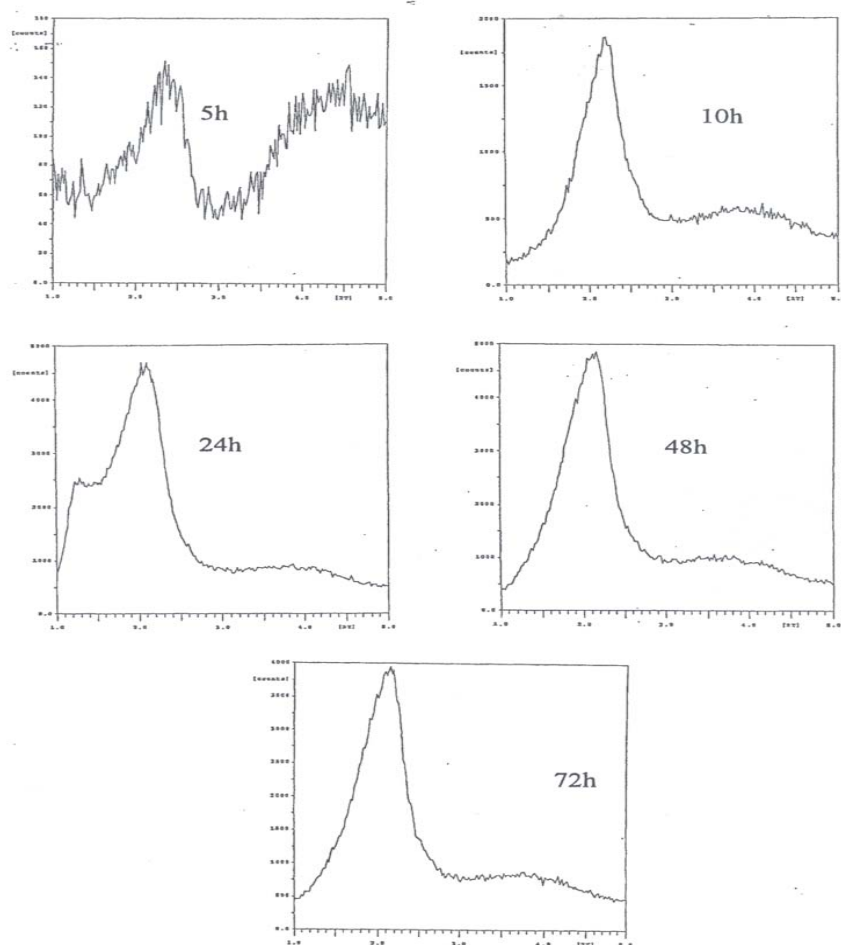


Figure 16: XRD patterns obtained for samples synthesized at various reaction times and fixed Al/P of 0.58 (2h mix before TMAOH)

4.1.5 Effect of reactants mixing time

The lack of hydrothermal stability is a considerable drawback in making the mesoporous aluminophosphates. Improvement in thermal stability may be achieved via an increase in pore wall thickness, which is related to extent of condensation within the pore walls. This experiment therefore, examines the effect of mixing time of the aluminum and phosphorous

precursors on the extent of hydrolysis and condensation. The reaction mixtures of the following molar compositions were used.

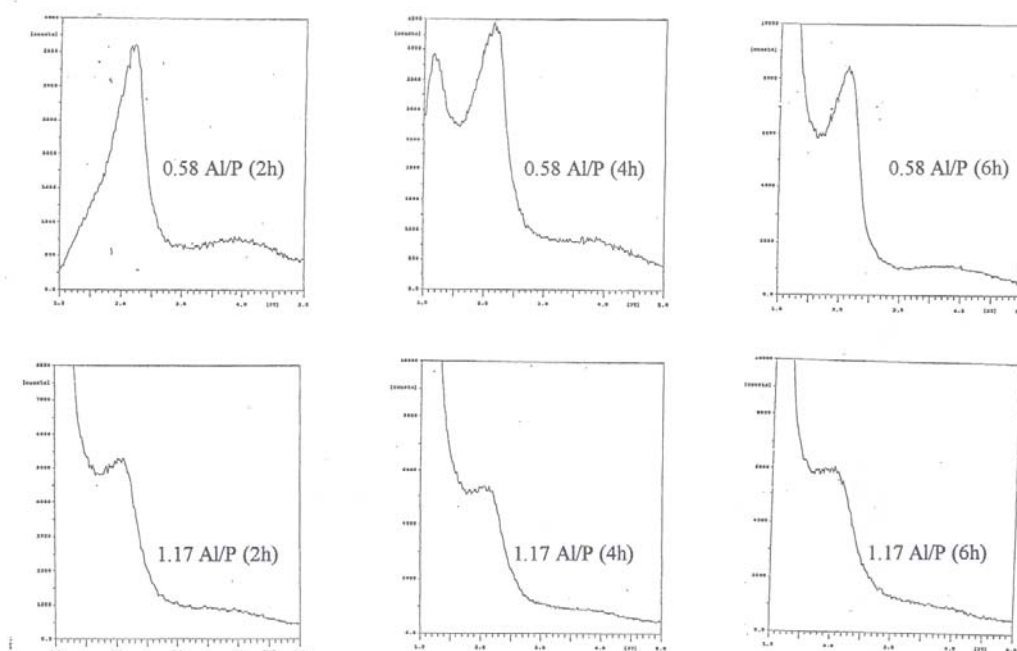
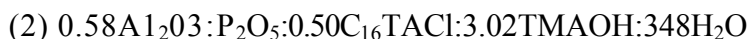


Figure 17: XRD of products obtained at various mixing times before TMAOH addition at Al/P= 0.58 and 1.17 (25°C)

XRD diffraction patterns from both ratios are shown in Figure 17. For samples with Al/P ratio = 0.58 a hexagonal phase was observed at 2 and 4 hrs mixing time, while a highly ordered hexagonal phase is obtained at 6 hrs mix time. Calcinations at 400°C for 1hr in N₂ of sample made from reactants mixing time of 2 hr, resulted in an amorphous product, while for the 4 and 6 hrs mixing time samples a broad low intensity peak was observed. The nitrogen isotherm and pore size distribution for Al/P = 0.58 is shown in Figure 18. Microporous (Type I) isotherm was exhibited for sample which were mixed for 4 and 6 hrs, while an isotherm was unattainable for the samples made from reactants mixing time of 2 hr. The pore

size distributions were however poorly defined for samples which were mixed for 4 and 6 hrs, possibly, due to a highly disordering of framework upon calcination.

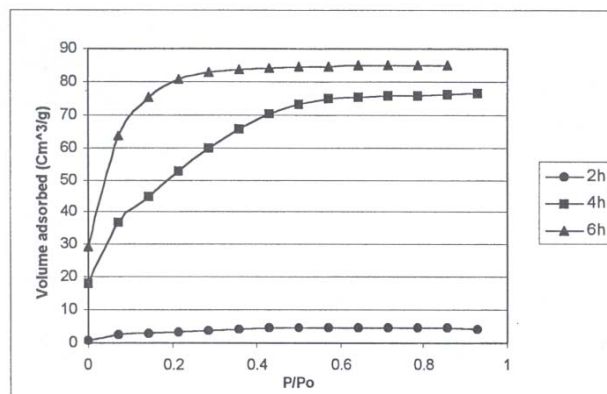


Figure 18: a) Adsorption isotherm for samples prepared with 2,4 and 6 hr mixing times

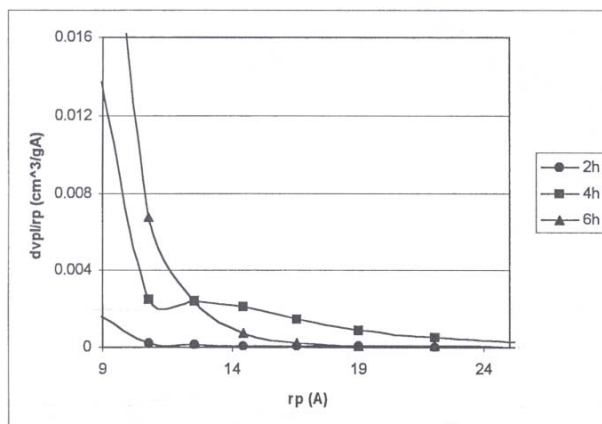


Figure 18b: Pore size distributions for samples made at various mixing times at Al/P ratio = 0.58.

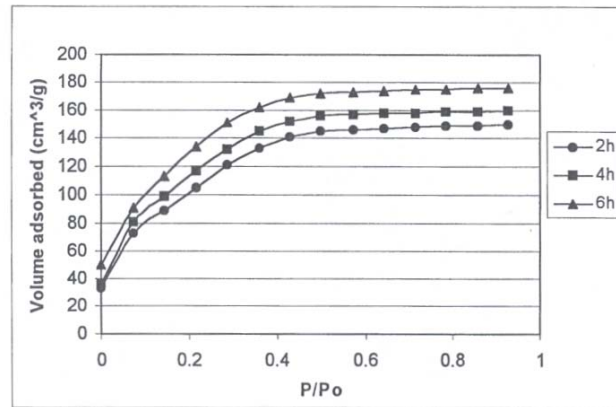


Figure 19a: Adsorption isotherms of samples made at various mixing times at A/P ratio 1.17

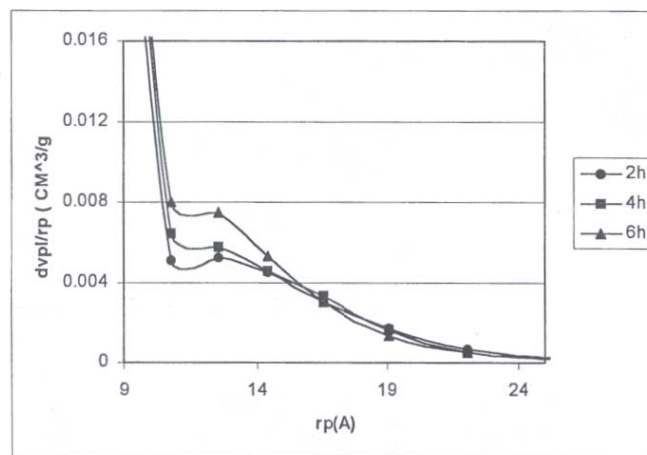


Figure 19 b: Pore size distributions of samples made at various mixing times at A/P ratio 1.17

For samples with Al/P ratio = 1.17, X-ray diffraction data indicated a similar hexagonal phase at 2,4 and 6 hr mixing times. The nitrogen isotherms and pore size distributions are shown in Figure 19. The isotherms for samples at 2,4 and 6 hrs indicate a microporous (Type I) nature as well, with no significant improvement in pore volume with increased mix time. The corresponding pore sizes indicate similar distributions for 2, 4 and 6 hr mixed time samples with a pore size of 12.6 Å.

Longer mixing time therefore resulted in an increase in pore volume. At higher Al/P ratio (1.17) pore size distribution indicates larger surface area and pore volume. At Al/P= 0.58 a highly disordered pore size distributions were noted for samples mixed for 4 and 6 hr, while for the 2h mix time sample, a pore size could not be determined.

4.2 Effect of aluminum source

It is well known that the choice of aluminum source plays a crucial role in the synthesis and phase purity of AlPO₄ molecular sieves.¹⁸ Although X-ray diffraction patterns and thermal analysis indicate mesoporous type material when using aluminumhydroxide, the materials lost crystallinity due to thermal instability. One of the factors thought to affect stability was the rate of hydrolysis and condensation of the inorganic species and the associated changes brought about. It was thought that different forms of aluminum would have different rates of hydrolysis and condensation. This was investigated further by varying aluminum isopropoxide and pseudoboehmite alumina.

4.2.1 Synthesis of mesoporous aluminophosphates at various using aluminum isopropoxide

4.2.1.1 Effect of Al/P ratio

In order to determine the effects of various aluminum content the composition of the starting mixtures was changed as follows: $x\text{Al}_2\text{O}_3:\text{P}_2\text{O}_5:0.50\text{C}_{16}\text{TMACl}:1.58\text{TMAOH}:349\text{H}_2\text{O}$, where

x was varied from 0.58 to 2.33, at 25 °C and mixing time varied at 2 and 6 hrs mixing time before TMAOH addition. The X-ray diffraction patterns for sample with Al/P ratio=0.58 and 6 hrs mix time are shown in Figure 20. The XRD patterns indicate that a low intensity peak corresponding to an intensity of 480 counts positioned at 2θ of 2.5° suggesting a hexagonal phase. However with an increase in synthesis Al/P ratio from 0.58 to 0.78 the hexagonal phase appeared to be highly disordered with lower intensity (150 counts). At Al/P ratio > 0.78 and up to 2.33, an amorphous product was observed. XRD patterns of products calcined at 400 °C for 3 hrs in nitrogen, shows a broad low intensity peak suggesting a highly disordered structure, due to loss in crystallinity. However, BET surface areas obtained at the various Al/P ratios ranged from 224 to 447 m²/g supporting the observation that the samples were partially stable under the calcinations conditions used. Nitrogen isotherms and pore size distributions for 21 hrs and 6 hrs mix time are shown in **Figures 21 and 22**. At Al/P ratios ranging from 0.58-2.33 intermediates between Types I and IV isotherms were observed for samples prepared from 2 hrs and 6 hrs mix time. The isotherm at 2 hrs mixing time exhibits a less steep pore filling in the relative pressure (P/P₀) range of 0.14 to 0.5, characteristic of capillary condensation into uniform mesoporous. The sharpness and height of capillary condensation (pore filling) step indicated in the isotherms is a measure of the pore size uniformity. The corresponding pore size distribution indicated that an increase in Al/P ratio from 0.58 to 1.17 resulted in an increase in pore size ranging from 14.4 to 19.0 Å and a broader distribution. At higher Al/P ratio (2.33) however, pore size was 16.5, but distribution was broader. The departures from a sharp and clearly defined pore filling step observed are usually an indication of increase in pore size heterogeneity (i.e. widening of pore size distribution).¹⁹ In addition the decrease in pore volume and surface area with an increase in Al/P ratio from 0.58 to 2.33 suggests that it may be due to a partial collapse of the hexagonal phase during calcination resulting from the instability associated with the presence of increasing amounts of framework aluminum.

Sample prepared with 6 hr mixing time, the nitrogen isotherms indicate an increase in pore volume as the Al/P ratio increases from 0.58 to 1.17. This increase in pore volume may be due to a prolonged mixing time, which gives the inorganic species ample time to hydrolyze and condense. The corresponding pore sizes distribution were narrow and ranged from 19.0 to 14.4 Å at Al/P ratios ranging from 0.58 to 1.17. However, for sample with at Al/P ratio 2.33, a broad distribution with a pore size of 25.9 Å.

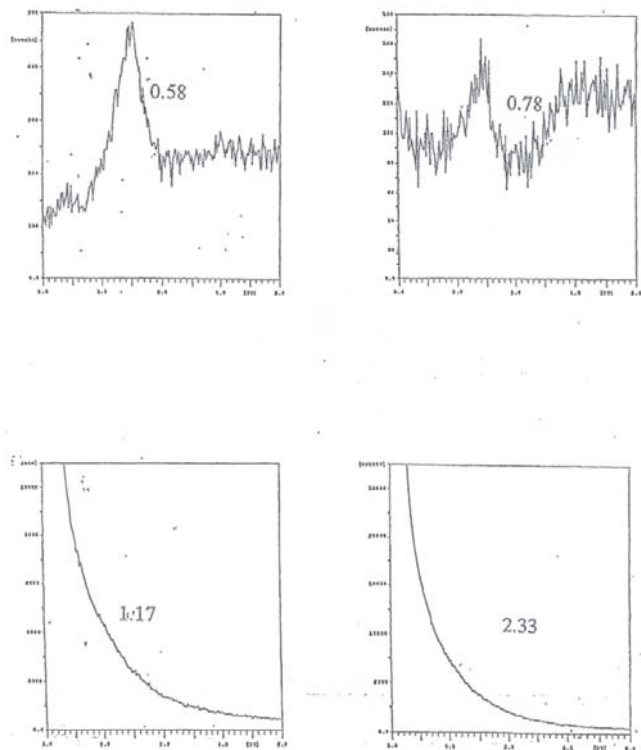
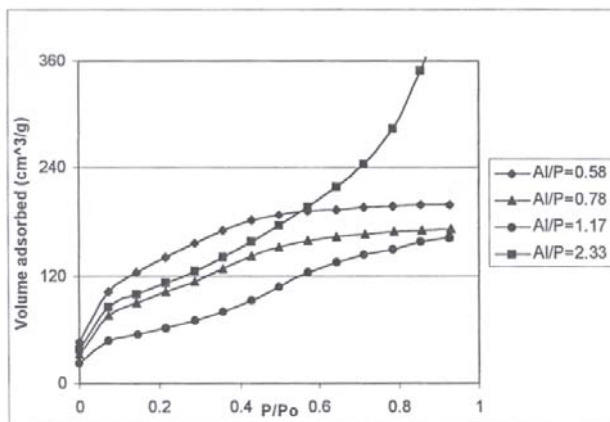
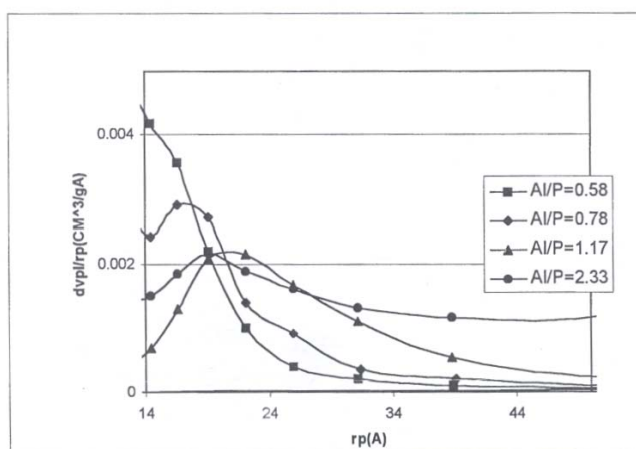


Figure 20: XRD patterns of samples synthesized with various Al/P ratios in mixture. (Al/P ratios on graph).

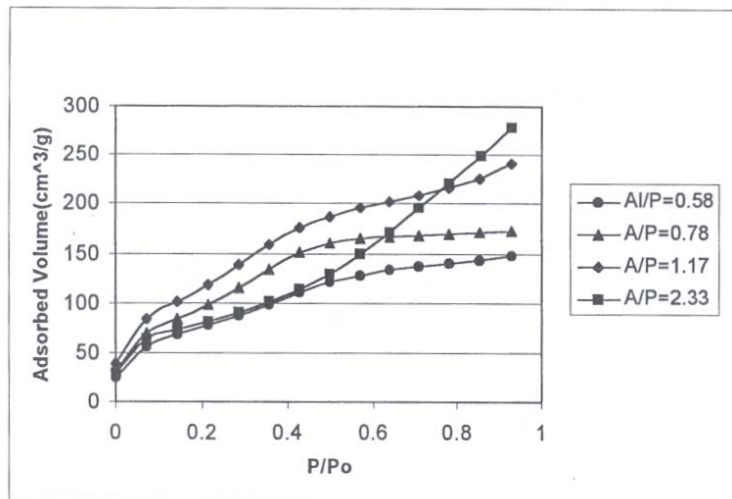


A) Adsorption isotherm

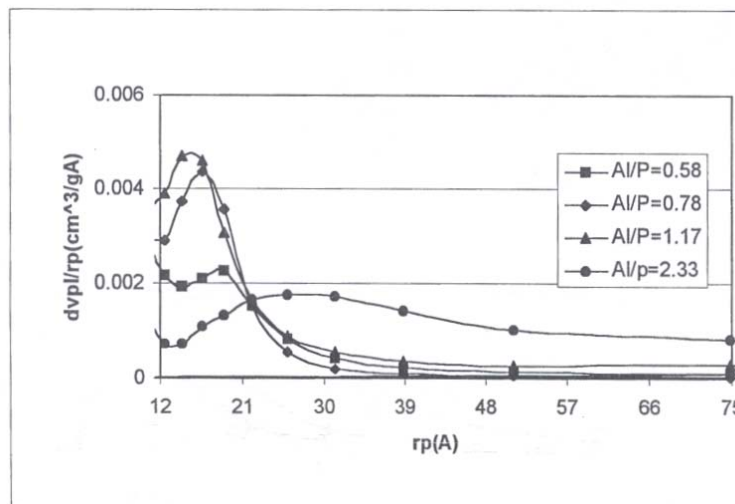


B) Pore size distribution

Figure 21: Adsorption isotherms A) and pore size distribution B) of samples synthesized with various Al/P ratios (2h mix time before TMAOH addition 25 °C)



A) Adsorption isotherm



B) Pore size distribution

Figure 22: Adsorption isotherms A) and pore size distribution B) of samples synthesized with various Al/P ratios (6h mix time before TMAOH addition, 25°C)

4.2.1.2 Effect of TMAOH concentration

Previously when using aluminum hydroxide it was noted that no mesostructured products were formed under the “TMAOH-free” condition. One of the roles of TMAOH is to act as a basic source to adjust the pH values of the starting mixtures. TMAOH also affects the solubility of the Al sources and or aluminophosphate species in the starting mixtures. Thus, it is of significance to investigate if TMAOH plays a similar role, as in the aluminum hydroxide synthesis. The molar compositions of the starting mixtures with Al/P ratios of 0.59 and 1.17 were changed as follows:

(1) $0.59\text{Al}_2\text{O}_3:\text{P}_2\text{O}_5:0.50\text{C}_{16}\text{TAC}1:x\text{TMAOH}:350\text{H}_2\text{O}$, where $x = 0.44\text{-}2.24$

(2) $1.17\text{Al}_2\text{O}_3:\text{P}_2\text{O}_5:0.50\text{C}_{16}\text{TAC}1:x\text{TMAOH}:350\text{H}_2\text{O}$, where $x = 0.32\text{-}3.06$

For sample synthesized with Al/P ratio = 0.59, and TMA/P₂O₅ = 0.44 (pH 4.1), X-ray diffraction pattern shows that (Figure 23) an amorphous product was obtained. At TMA/P₂O₅= 0.52 (pH 7.09) a lamellar phase was obtained. With an increase in TMA/P₂O₅ from 1.08 to 2.24 (pH 10.81 and 11.15) however, a hexagonal phase was observed. At higher Al/P ratio (1.17) (**Figure 24**) an amorphous phase was obtained at TMA/P₂O₅ ranging from 0 to 0.32 (pH 4.13 to 7.00) and a hexagonal phase with low crystallinity was observed at TMA/P₂O₅= 0.32 (pH 9.66). An increase in TMA/P₂O₅ to 3.06 (pH 11.27) resulted in a broad, highly disordered hexagonal phase. A lamellar phase was not obtained at this ratio.

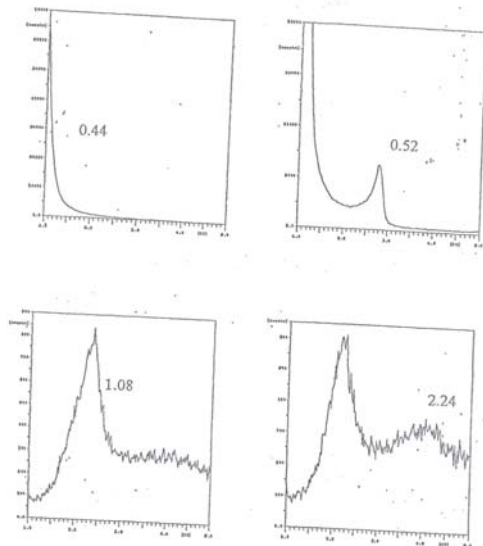


Figure 23: XRD patterns of products obtained from synthesis mixtures of various TM A/P₂O₅ ratios and fixed Al/P of 0.59 (synthesis conducted at 25°C) (TMA/P₂O₅ratio as indicated on graph)

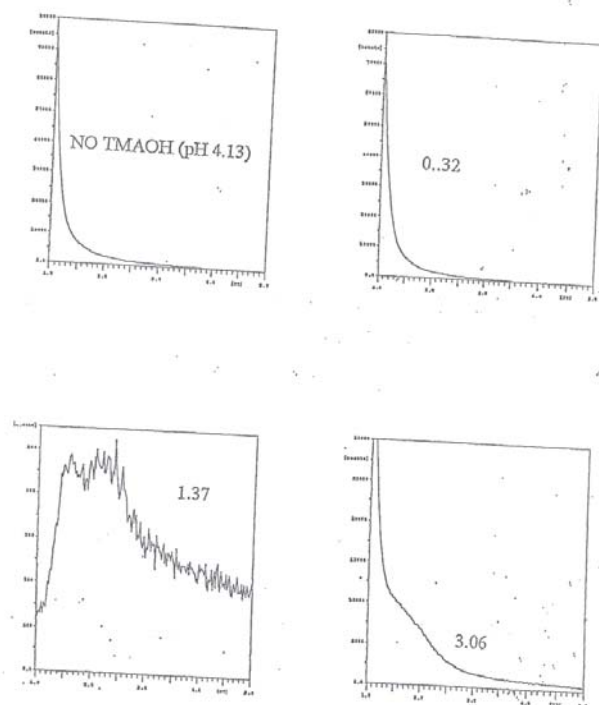


Figure 24: XRD patterns of products obtained from synthesis mixtures of various TM A/P₂O₅ ratios and fixed Al/P of 1.17 (synthesis conducted at 25°C) (TM A/P₂O₅ ratio as indicated on graph)

4.2.1.3 Effect of surfactant concentration

Synthesis mixtures with Al/P ratios of 0.58 and 1.16 and varying amounts of C₁₆TACl were prepared with the following molar compositions:

(1) 0.58 Al₂O₃:P₂O₅:x C₁₆TACl:3.44 TMAOH:349H₂O, where x = 0.24-0.74

(2) 1.16Al₂O₃:P₂O₅:x C₁₆TACl:1.80TMAOH:347H₂O, where x = 0.24-0.74

X-ray diffraction patterns (**Figure 25**) of products synthesized at 25°C and Al/P ratio 0.58, show that increase in CTACl/P₂O₅ ratio from 0.24 to 0.32 gave a hexagonal phase with improved crystallinity. Similar trends were observed at 110°C synthesis temperature at CTACl/P₂O₅= 0.74 however, a less ordered hexagonal phase was observed. In **Figure 26** synthesis using the higher Al/P ratio (1.16) conducted at 25°C, resulted in amorphous product for CTACl/P₂O₅ ranging between 0.24 and 0.74. Similar trends were observed at 110°C synthesis ranging between 0.24 and up to 0.74 CTACl/P₂O₅= 0.74 however, lamellar phase was obtained.

Both Al/P ratios indicated that high surfactant content and elevated temperature resulted in a lamellar phase while lower surfactant and lower temperature favors a hexagonal phase.

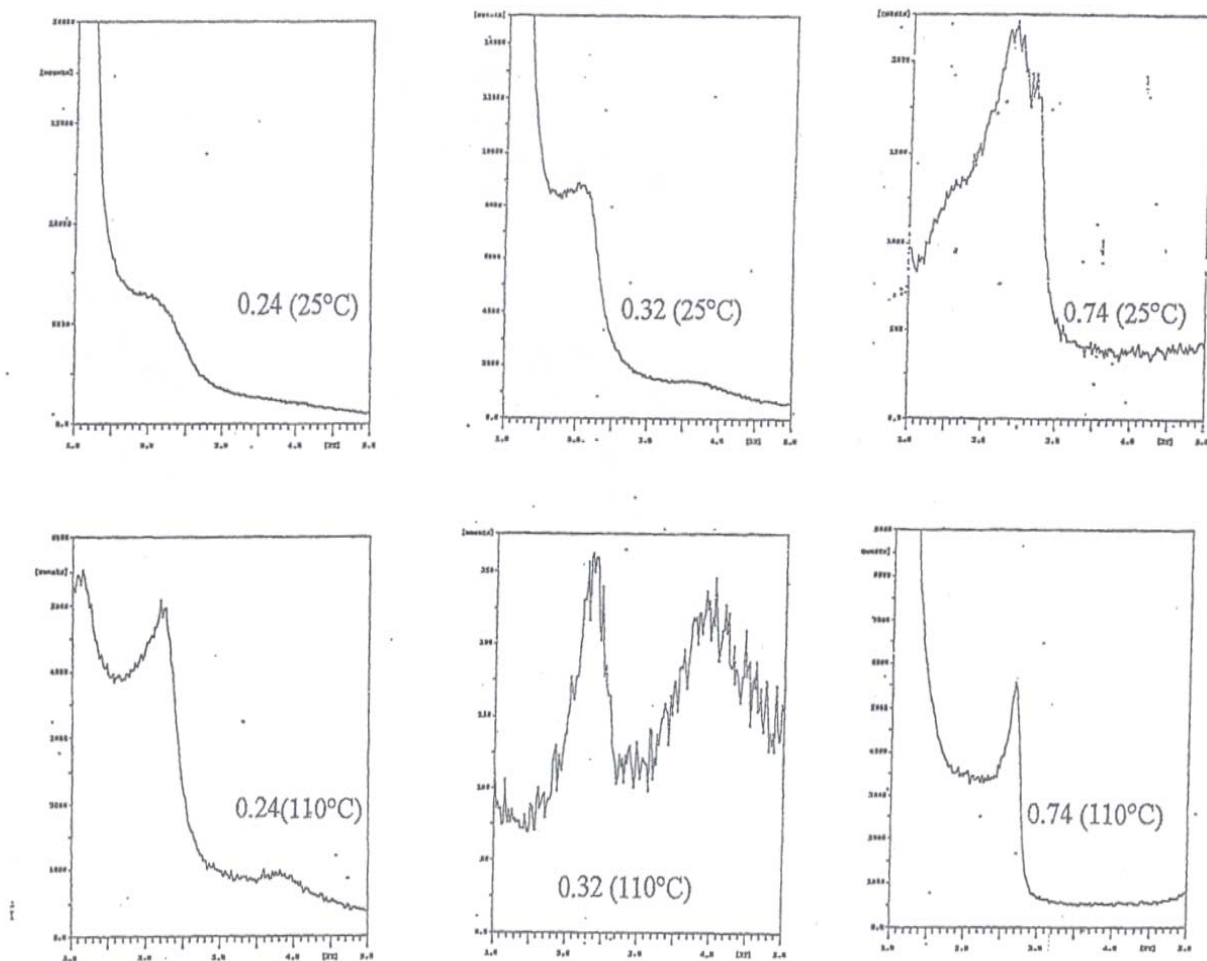


Figure 25: XRD patterns of products obtained from synthesis mixtures of various CTACl/P₂O₅ ratio and fixed Al/P of 0.58 (synthesis, conducted at 25°C and 110°C).

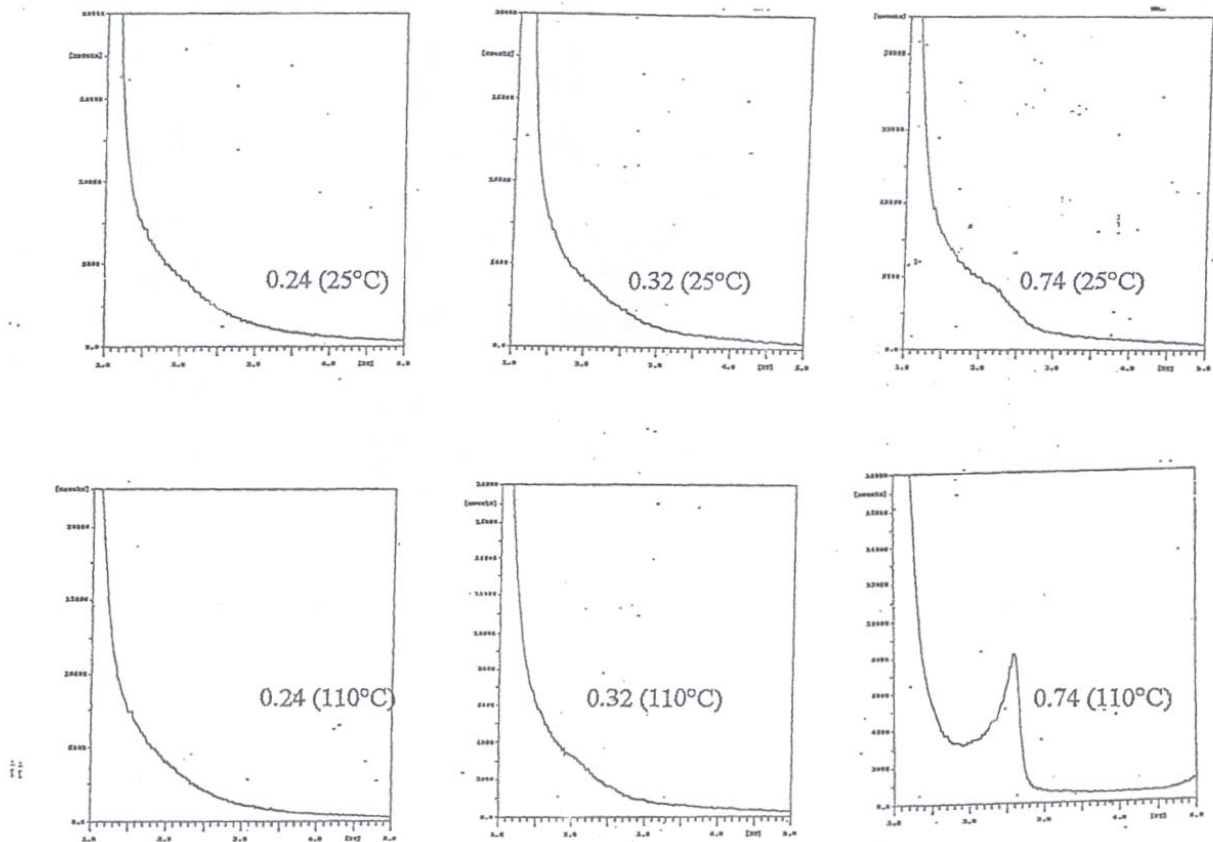


Figure 26: XRD patterns of products obtained from synthesis mixtures of various CTACl/P₂O₅ ratio and fixed Al/P of 1.16 (synthesis conducted at 25°C and 110°C)

4.2.1.4 Effect of water concentration

Using Al/P ratios of 0.58 and 1.15, the following molar compositions were prepared to study the effects of water content.

- (1) 0.58Al₂O₃:P₂O₅:0.50C₁₆TACl:2.30TMAOH:w H₂O, where w = 86-689
- (2) 1.15Al₂O₃:P₂O₅:0.48C₁₆TACl:1.48TMAOH:wH₂O, where w = 85-687

For samples with Al/P ratio= 0.58 synthesized at 25°C, **Figure 27** shows X-ray diffraction patterns obtained for H₂O/P₂O₅ ratios ranging from 86 to 689. At H₂O/P₂O₅ ratio 86 a hexagonal phase was obtained and with an increase in H₂O/P₂O₅ ratio from 349 to 689 a hexagonal phase with low crystallinity was obtained. An increase in Al/P ratio to 1.15 (**Figure 28**) resulted in a hexagonal phase at H₂O/P₂O₅ ratios of 85 and 172 and a decrease in hexagonal product quality resulted at 344 H₂O/P₂O₅. At an increased H₂O/P₂O₅ ratio of 687 a highly disordered diffraction pattern is obtained. The nitrogen isotherms and pore size distributions for Al/P ratio= 0.58 (**Figure 29**) indicate an intermediate between Type I and IV. The corresponding pore size distributions was 16.5Å at H₂O/P₂O₅ ratio 689, while a definite pore size could not be obtained for H₂O/P₂O₅ ratio < 689. The nitrogen isotherms and pore size distribution (**Figure 30**) for Al/P ratio of 1.15 indicates a Type IV isotherm at H₂O/P₂O₅ ratios 172 and 344, while an intermediate between Type I and IV was exhibited for H₂O/P₂O₅ ratio 86. A narrow pore size of 14.4Å was observed for H₂O/P₂O₅ ratio = 86, while an increase in water content to ratio of H₂O/P₂O₅ = 344 resulted in a broad pore size distribution with a pore size of 19.0 Å. Himyak *et.al* reported that synthesis with low water concentration involves a viscous mixture with no clear separation between solution and the product. High water content enhances molecular transport within the reaction medium resulting in a more crystalline material. Our results however indicate that the mixtures with high water content form materials with low crystallinity. Therefore, even the mixtures with low water content provide sufficient transport properties for the formation of a highly crystalline material.

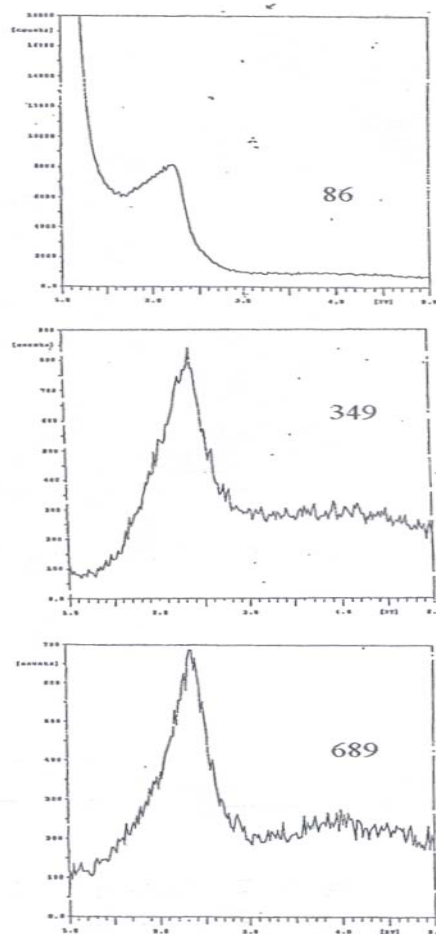


Figure 27: XRD patterns of product synthesized with various water content and Al/P = 0.58, 25°C; 0.58 Al₂O₃: P₂O₅: 0.50 C₁₆TACl: 2.30 TMMAOH: w H₂O, where w = 86-689

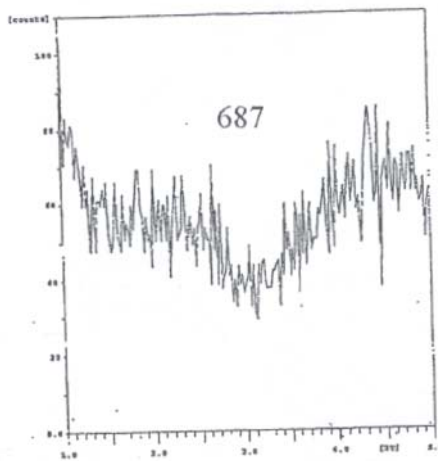
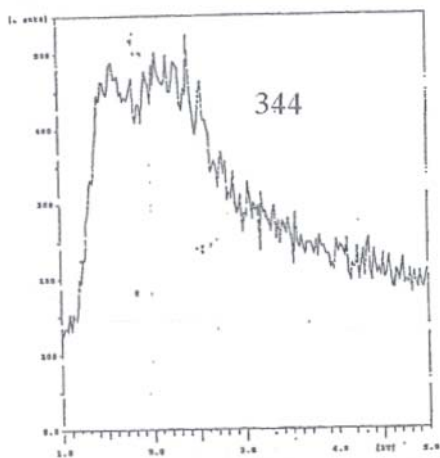
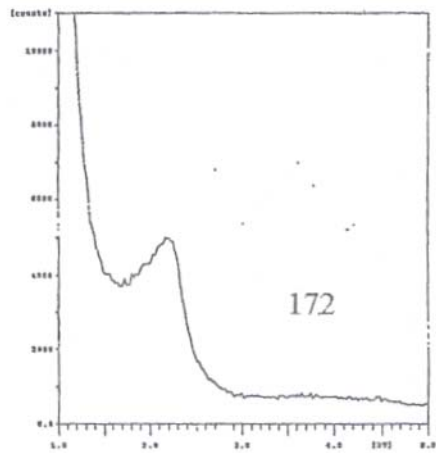
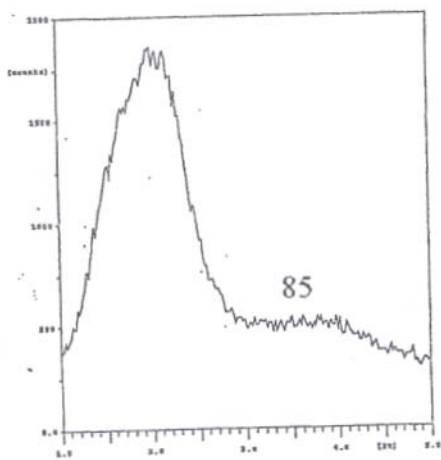
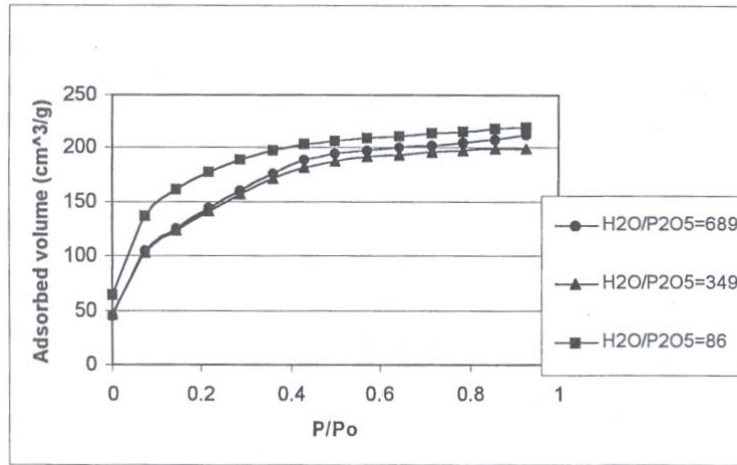
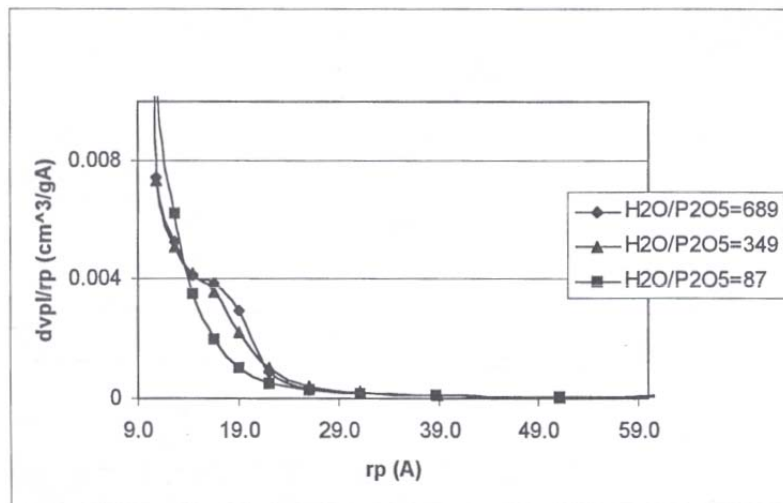


Figure 28: XRD patterns of product synthesized with various water content and Al/P = 1.15.15Al₂O₃:P₂O₅:0.48 C₁₆TACl: 1.48TMAOH: wH₂O, where w = 85-687

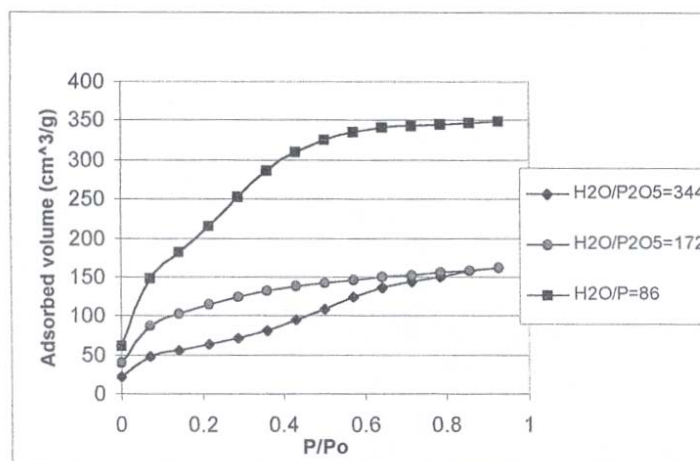


A) Adsorption isotherm

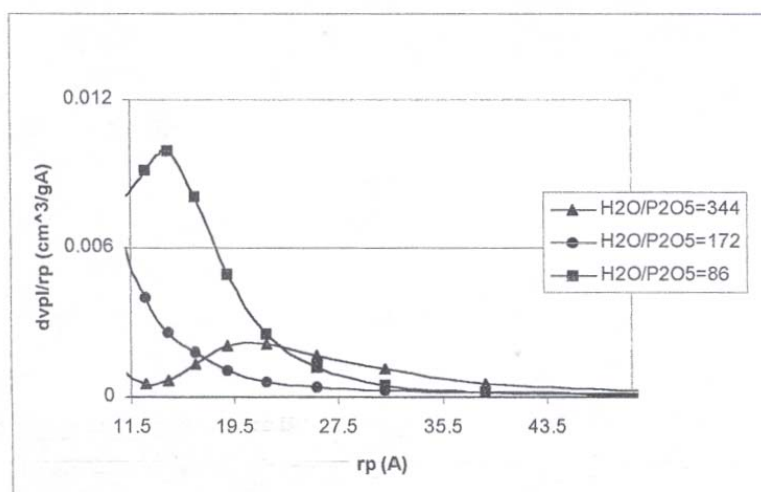


B) Pore size distribution

Figure 29: A) Adsorption isotherm and B) Pore size distribution of samples synthesized with various water concentration and Al/P= 0.58 Al/P (25 °C)



A) Adsorption isotherm



B) Pore size distribution

Figure 30: A) Adsorption isotherm and B) Pore size distribution of samples synthesized with various water concentration and Al/P= 1.15 (25°C)

4.3 Synthesis of mesoporous aluminophosphates using Pseudoboehmite alumina

Changing the aluminum source from aluminum hydroxide to aluminum isropoxide was found to have significant impact on the products obtained. This therefore prompted further investigation using a third source of aluminum (Pseudoboehmite alumina).

4.3.1 Effect of various Al/P ratios

The effect of Al/P ratios was investigated using reaction mixtures of molar compositions $x\text{Al}_2\text{O}_3:\text{P}_2\text{O}_5:0.50\text{C}_{16}\text{TAC}1:2.98\text{TMAOH}:350\text{H}_2\text{O}$, where $x= 0.59-2.34$. For synthesis with Al/P ratio of 0.59 and 0.77 and 25°C , the X-ray diffraction data (**Figure 31**) indicates a hexagonal phase with low crystallinity, as evidenced by a broad low intensity peak: of 2θ at 2.1° . An increase in synthesis Al/P ratio to 1.17 resulted in a very disordered product, while Al/P ratio = 2.34 an amorphous product was obtained. Comparing the pseudoboehmite alumina x-ray diffraction patterns at various Al/P ratios to aluminum hydroxide indicated products with less crystallinity, but higher surface area and pore size were produced using the former aluminum source.

Calcination at 400°C of the products from Al/P ratios 0.59 to 2.34, resulted in product loss at all Al/P ratios, except for Al/P ratio= 0.77, where crystallinity was partially preserved. Although materials appeared to have lost their crystallinity on calcination, surface area and porosimetry analysis showed that a mesoporous material of relatively high surface areas were still present at synthesis with Al/P ratios = 0.59, 1.17 and 2.34 the corresponding nitrogen isotherms and pore size distribution are shown in (Figures 32A and B). Type IV isotherms were obtained for Al/P= 0.59, 1.17 and 2.34 while a combination of Type I and IV were observed for synthesis with Al/P ratio = 0.77, where an inflection (pore filling) occurred over a broad range of relative pressure. A broad distribution with a pore size of 31.2: was exhibited for Al/P ratios 0.59 and 0.77, while a narrower distribution was obtained for Al/P ratio =1.17. At Al/P ratio= 2.34 a narrow distribution with a pore size of 25.9\AA was obtained. For higher reaction temperature synthesis 110°C and Al/P ratio = 0.59, the X-ray diffraction patterns (**Figure 33**) shows a hexagonal phase, while Al/P ratio > 0.59 and up to 2.34 amorphous products were observed. The nitrogen isotherms (**Figure 34**) indicate an intermediate between Types I and IV for Al/P ratio = 0.59, while a Type IV isotherm was obtained between Al/P ratios of 0.77 and 2.34.

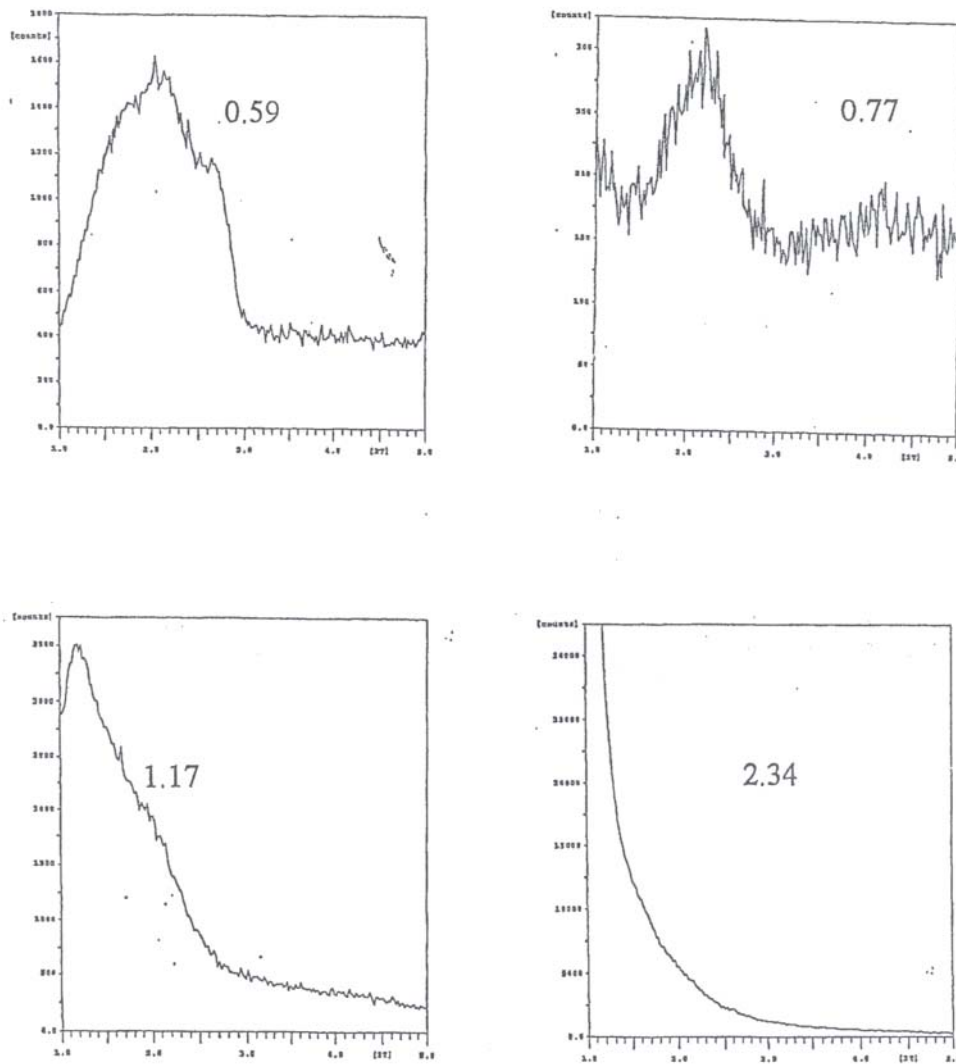
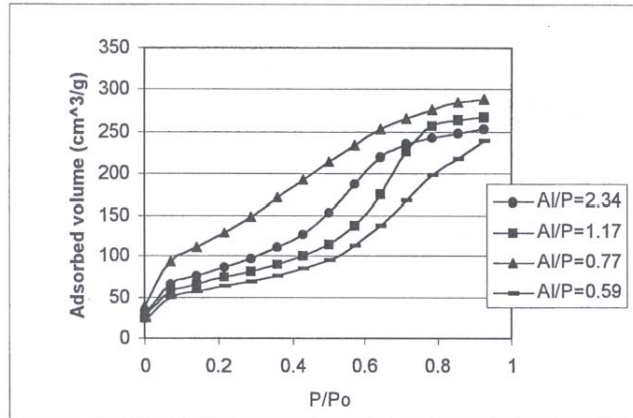
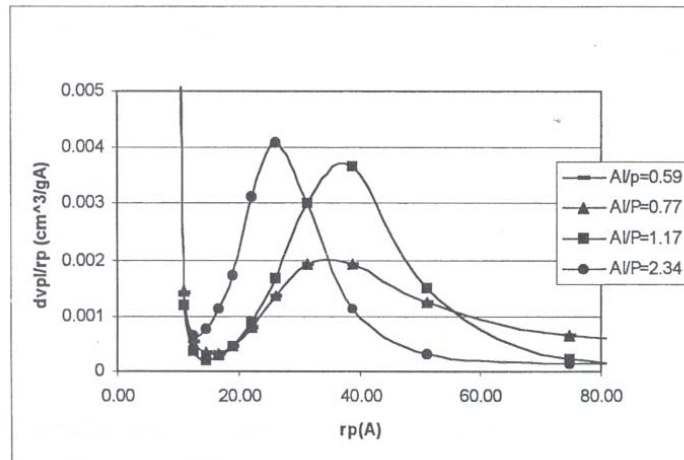


Figure 31: XRD patterns of samples synthesized at various Al/P ratios in mixture (synthesis conducted at 25°C, Al/P ratio indicated on graph)



A) Adsorption isotherms



B) Pore size distribution

Figure 32: A) Adsorption isotherms and B) Pore size distribution of samples synthesized under various Al/P ratio in the presence of Psuedoboehemite alumina at (25°C)

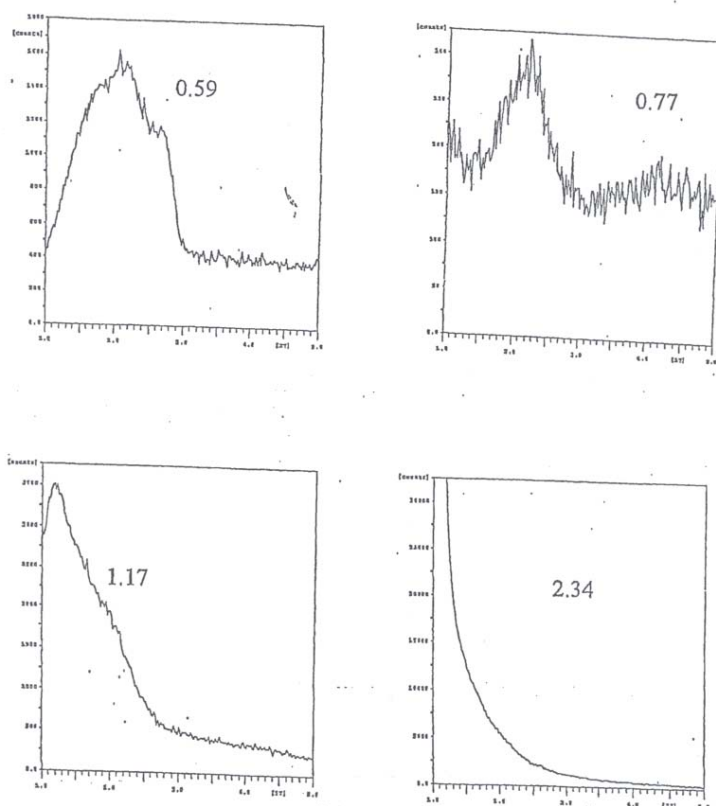


Figure 33: XRD patterns of samples synthesized at various Al/P ratios in mixture (synthesis conducted at 110°C) (Al /P ratio indicated on graph)

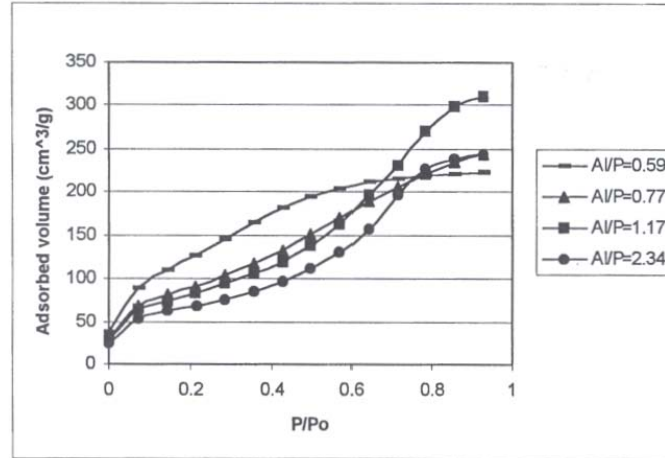


Figure 34: Adsorption isotherm of calcined samples synthesized at various Al/P ratios in mixture (synthesis conducted at 110°C)

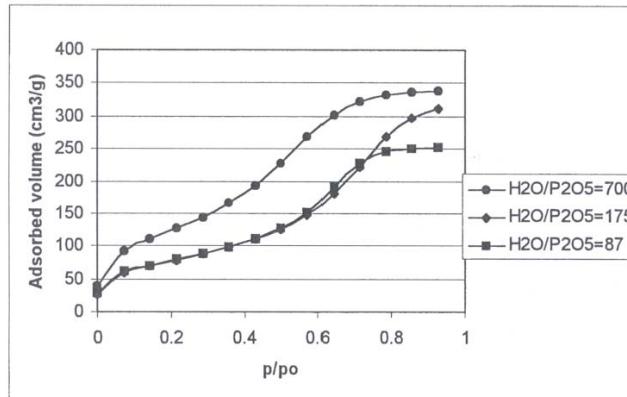
4.3.2 Effect of water concentration

Molar compositions containing varying amounts of water were prepared for Al/P ratios of 0.58 and 1.17 as follows:

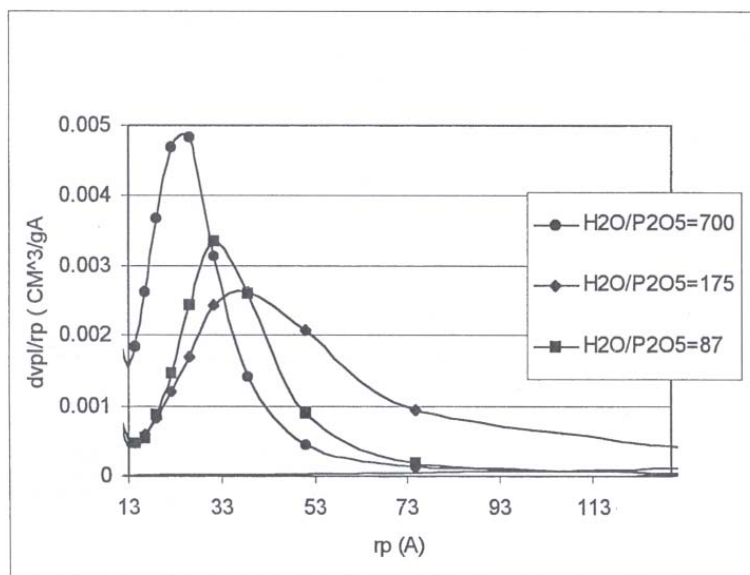
- (1) $0.58\text{Al}_2\text{O}_3:\text{P}_2\text{O}_5:0.50\text{C}_{16}\text{TAC}1:3.26 \text{ TMAOH}:x\text{H}_2\text{O}$, where $x= 87-700$
- (2) $1.17\text{Al}_2\text{O}_3:\text{P}_2\text{O}_5:0.50\text{C}_{16}\text{TAC}1:3.22 \text{ TMAOH}:x\text{H}_2\text{O}$, where $x= 87-700$

Previously aluminum isopropoxide indicated that the water content of the synthesis mixture was an important structure directing parameter. Hence it was instructive that water content in the pseudoboehmite system be further explored. The nitrogen isotherm and pore size distribution are indicated in (Figure 35) for Al/P ratio 1.17 at 25°C. A type IV isotherm was exhibited at H₂O/P₂O₅ ratios 87.0 to 700. The pore size analysis indicates a narrow distribution with a maximum centered around 22 Å for H₂O/P₂O₅ ratio= 700. A broad distribution were observed for H₂O/P₂O₅ ratio = 175 with a pore size of 38.8 Å and for H₂O/P₂O₅ ratio = 87.0 with a pore size of 31.2 Å. For Al/P ratio = 0.58 (Figure 36) a Type IV isotherm, similar to Al/P ratio 1.17, was obtained. The corresponding pore sizes at H₂O/P₂O₅ ratio= 172 and 700 resulted in a broad distribution with a pore size of 25 Å while at H₂O/P₂O₅ ratio= 87, a pore size of 22.04 Å is obtained. For Al/P ratios = 1.17 synthesized at 110°C (Figure 37) a Type IV isotherm for

H₂O/P₂O₅ ratios = 174 and 700 was obtained while an intermediate isotherm between Type I and IV was obtained at H₂O/P₂O₅ ratio= 175. The pore size distribution corresponding to the isotherms showed a narrow distribution with a pore size of 31.2Å for H₂O/P₂O₅ ratio = 700, while a pore size of 16.5Å and 38.8Å was determined for H₂O/P₂O₅=175.0 and 87.0 respectively. Samples from synthesis at higher temperatures (110°C) using Al/P ratio = 0.58 (**Figure 38**) show broad distribution with a pore size of 25Å at H₂O/P₂O₅ ratio = 172 and 700 while a 31.2 Å pore size was obtained at H₂O/P₂O₅ ratio of 87

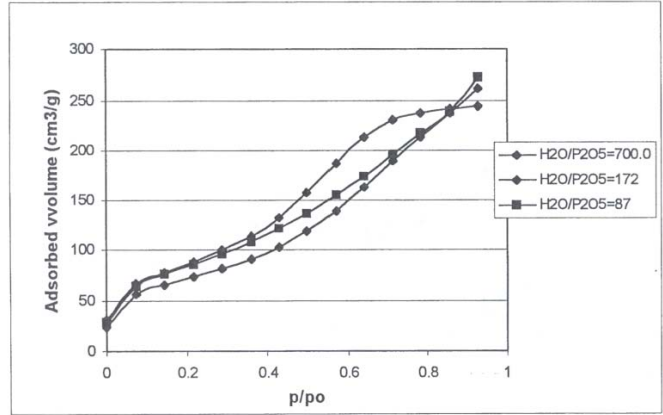


a) Adsorption isotherm

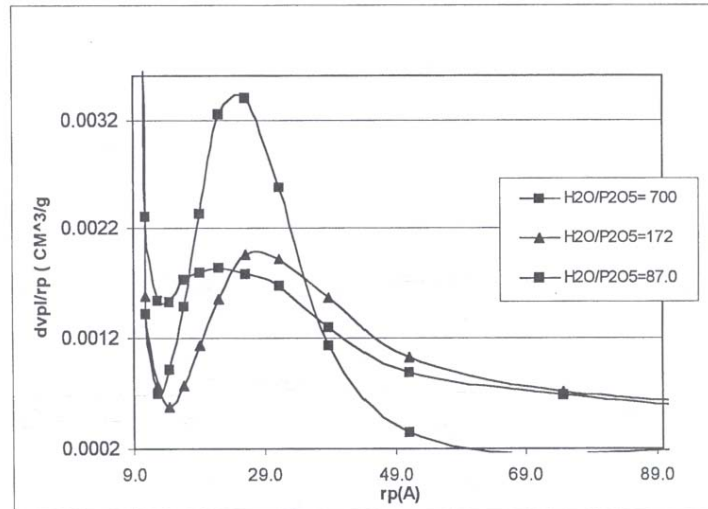


b) Pore size distribution

Figure 35: a) Adsorption isotherm and b) pore size distribution of calcined samples synthesized at various water content in mixture in mixture (Al/P ratio 1.17, synthesis conducted at 110°C)

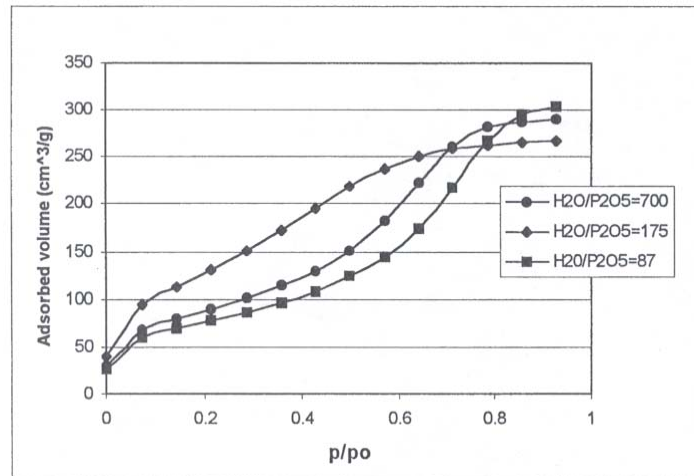


a) Adsorption isotherm

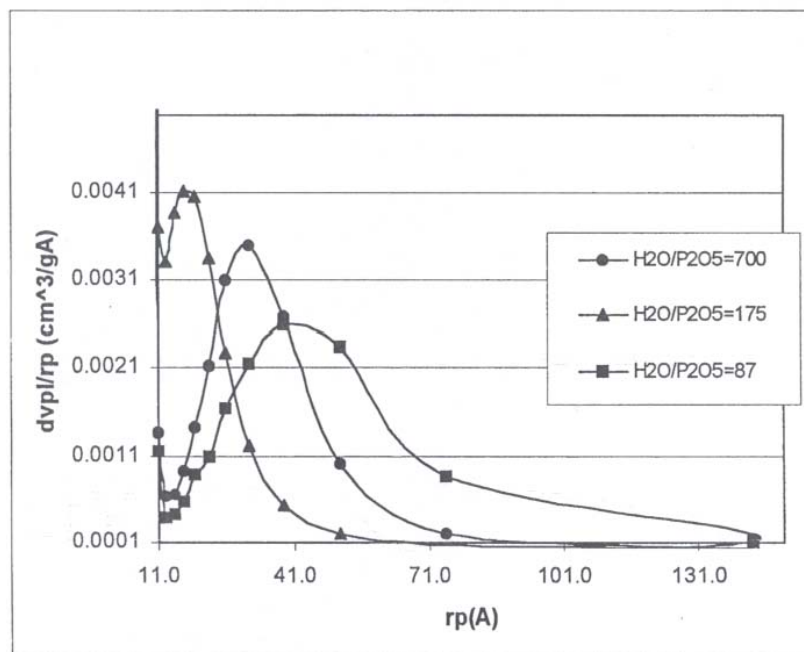


b) Pore size distribution

Figure 36: a) Adsorption isotherm and b) pore size distribution of calcined samples synthesized at various water content in mixture in mixture (Al/P ratio 0.58, synthesis conducted at 25°C)

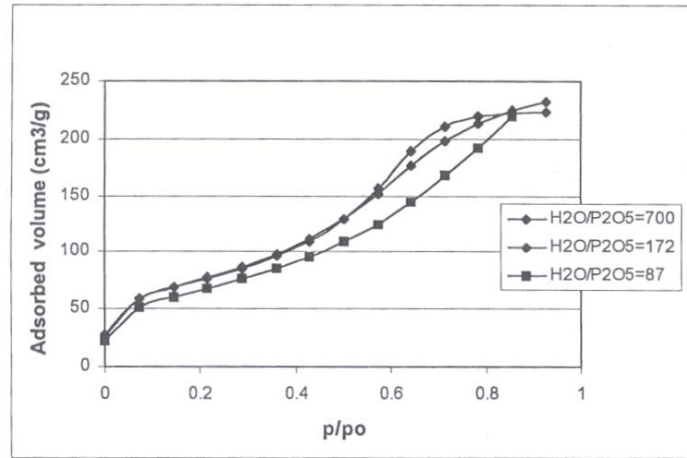


a) Adsorption isotherm

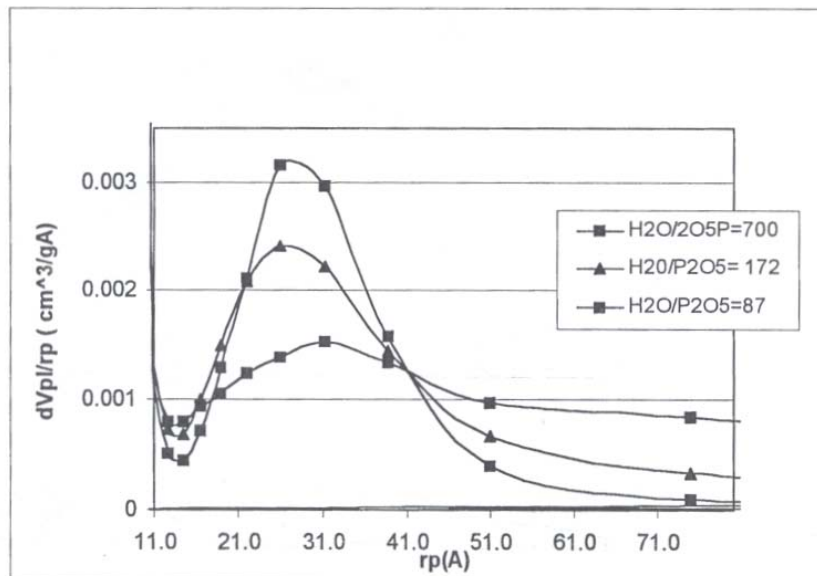


b) Pore size distribution

Figure 37: a) Adsorption isotherm and b) pore size distribution of calcined samples synthesized at various water content in mixture in mixture (Al/P ratio 1.17 Al/P, synthesis temperature 110°C)



A) Adsorption isotherm



B) Pore size distribution

Figure 38 : A) Adsorption isotherm and B) pore size distribution of calcined samples synthesized at various water content in mixture in mixture (Al/P ratio 0.58, synthesis temperature 110°C)

4.4 Synthesis of Aluminophosphate containing Mg and Cobalt

Magnesium and cobalt containing AlPOs were synthesized using using procedure outlined in section 3.2.3.3 below and except that magnesium and

cobalt salts were added in the form of the dissolved acetate salts. Like the case of the pure AlPO_4 , XRD patterns of the samples show a single peak around 2θ of 2° , indicating some degree of structural ordering the samples (**Figure 39**). On calcination at elevated temperature however, this peak is significantly reduced and broadened or disappears, signaling structural degradation or total collapse.

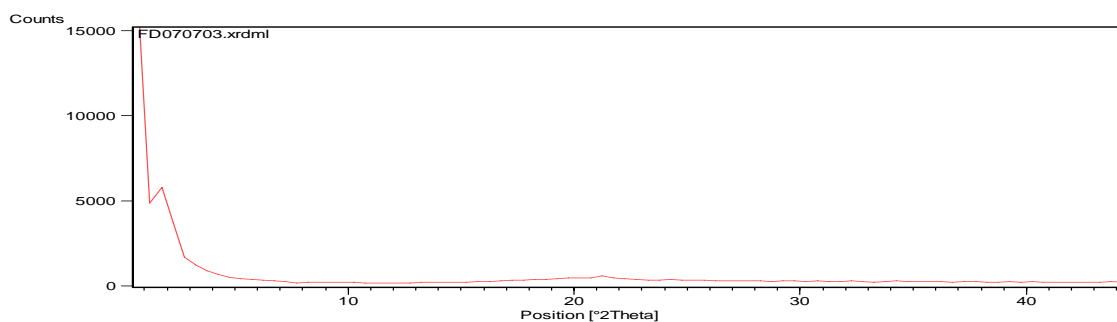
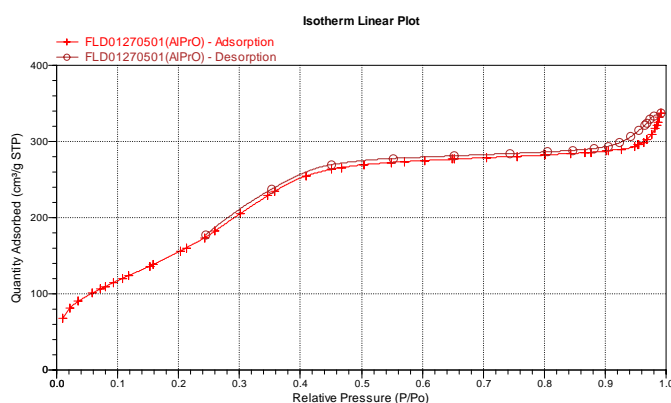


Figure 39. XRD of “As-synthesized” cobalt containing mesostructured AlPO sample

The calcined (only at 350°C in nitrogen) samples however showed high surface area ($\sim 600 \text{ m}^2/\text{g}$) with with BJH pore size of 3.2 nm. Adsorption-desorption isotherms were combinations of Type I and IV, showing that the samples had some degree of mesoporosity (**Figure 40**). Their thermal stabilities at higher temperatures were not evaluated.



PURE AlPrO
BET Surface area:
596 m²/g

Pore volume:
0.496cm³/g

Figure 40. Adsorption-desorption isotherms of calcined cobalt containing mesostructured AlPO_4 sample

Calcined (only at 350°C in nitrogen) aluminophosphates synthesized with the following organics added to the synthesis mixtures (1,2 bis-trimethoxysilylethane labeled as BTSE, 3-mercaptopropyltriethoxysilane, labeled as -SH, 3-aminopropyltriethoxysilane labelled –NH, and propyltriethoxysilane, labeled as Propyl) to be incorporated as part of the pore walls structure or be grafted by silane linkages, also showed high surface areas up to 725 m²/g, and pore size between 2.22 and 3.88 nm (**Figures 41 to 43**). However these organo-aluminophosphate mesoporous materials, though not of immediate catalytic applications, can be further explored for the incorporation of other divalent metals to impart acid sites and other catalytic sites. These samples were synthesized at the end of this project and were not evaluated and fully characterized, and therefore will be the subject of future investigations.

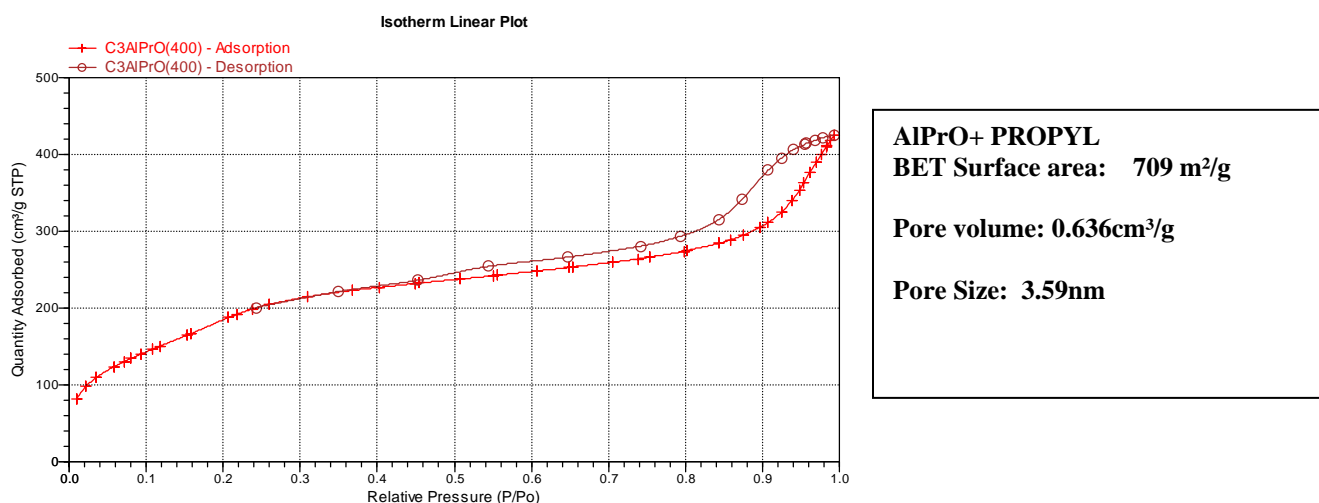


Figure 41. Adsorption-desorption isotherms of calcined mesoporous organo-aluminophosphate synthesized in the presence of propyltriethoxysilane

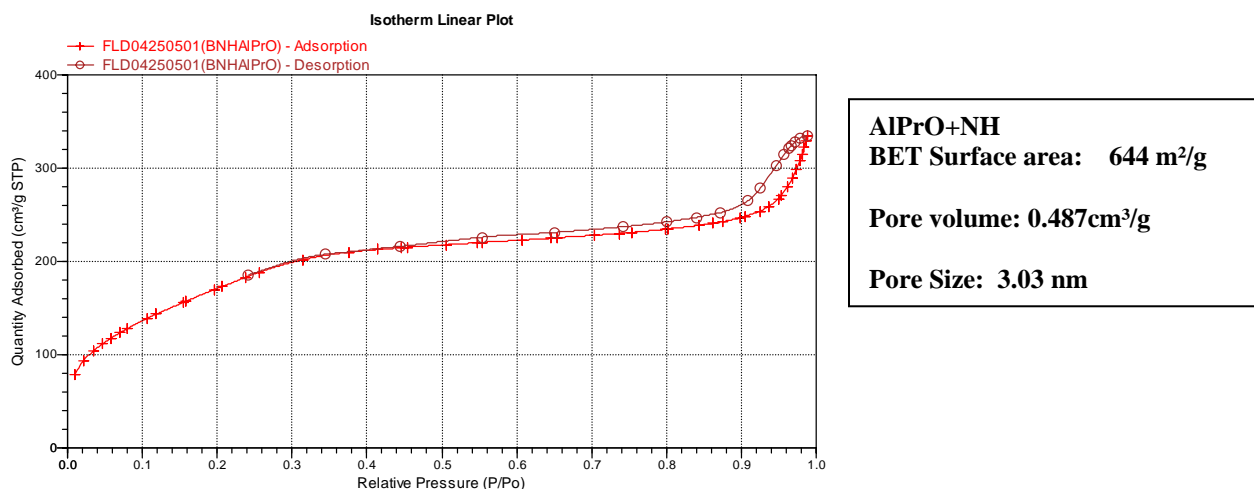


Figure 42. Adsorption-desorption isotherms of calcined mesoporous organo-aluminophosphate synthesized in the presence of 3-aminopropyltriethoxysilane

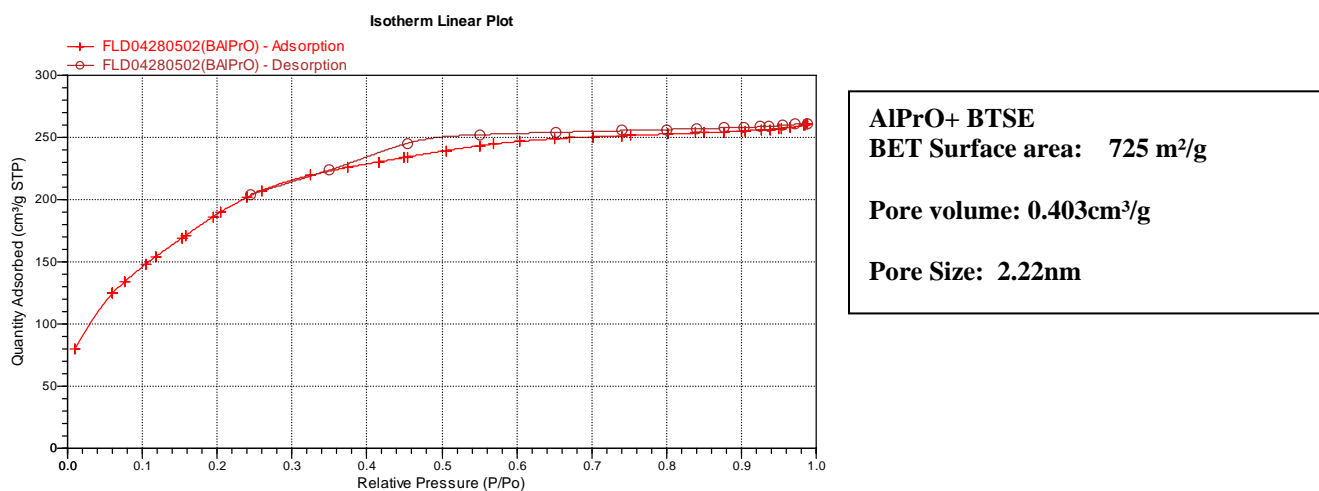


Figure 43. Adsorption-desorption isotherms of calcined mesoporous organo-aluminophosphate synthesized in the presence of 1,2 bis-trimethoxysilyl ethane

4.5 Catalytic screening

Calcined samples of mesoporous aluminophosphates and cobalt and magnesium containing aluminophosphates, among those that showed high surface areas and mesoporosity described in the previous section, were evaluated for the conversion of cumene (as a probe reaction) in a continuous flow catalytic reactor. Their catalytic activities were compared with a commercial catalyst, namely zeolite Y. The samples showed no conversion of cumene up to 350°C. Further investigation will be necessary to evaluate the presence/absence and nature of the catalytic sites. Due to the absence of catalytic activities for these samples, no heavy oil upgrading evaluation were conducted, or will be conducted until improvements in the thermal stability and catalytic properties of the materials are achieved.

5. CONCLUSIONS

Mesoporous aluminophosphates were synthesized from a reactive gel via a liquid crystal templating mechanism in the presence of a cationic surfactant, CTACl. The synthesis of these materials were performed at various molar compositions. The choice of aluminum source is crucial in the type and quality of the products formed. Lamellar and hexagonal phases can be directed by altering the composition of the starting mixtures or the synthesis temperature irrespective of the three aluminum sources investigated. Low Al/P ratio, low TMAOH, high CTACl and high temperature led to a lamellar phase by facilitating condensation of inorganic precursors, while high Al/P ratio, high TMAOH, low CTACl and lower temperature led to a hexagonal phase.

However, most ordered mesostructured products were obtained using aluminum hydroxide as aluminium source. Synthesis in the presence of aluminum hydroxide gave a highly ordered mesoporous type materials with Al-O-P species in predominantly tetrahedral coordination in the lamellar phase and both tetrahedral and octahedral coordination in the hexagonal phase. Upon calcination a collapse or substantial shrinkage of the framework resulted. Synthesis with psudeobohemite alumina however gave a Type IV isotherm indicating mesoporosity with a pore size of up to 39 Å and varied with water content. A micro-meso type porous material was obtained in the presence of aluminum isopropoxide with a pore size in the range of 19 Å. Mesoporous aluminophosphates synthesized as pure AlPO_4 or with organosilanes as components of the ordered structures (added during condensation) maintained mesoporous structures, high surface areas up to 600 m^2/g and pore volume and uniform pore sizes up to 36 Å, after calcination in nitrogen at 350°C.

6. FUTURE WORK

The mesoporous lamellar and hexagonal phases of aluminophosphate were produced, but with varying degrees hydrothermal instability and low crystallinity. The latter present considerable drawbacks for their use as catalysts and therefore, there are alternative methods to improve these physicochemical characteristics are needed. Further studies on the extent of hydrolysis and condensation of inorganic precursors and their impact on product stability is needed. One of the areas to look for improvement also, is the SBA type materials from the silicate system which have high thermal stability as well as large surface area. As indicated in our study the choice of surfactants amongst other factors is crucial. The use of the block co-polymers as surfactants to synthesize the SBA type materials which help to assist in pore expansions can also be implemented in the aluminophosphate system. It is also believed that co-block polymers can increase pore wall thickness, hence their usage to improve the thermal stability of aluminophosphates is of interest for further investigation.

7. LIST OF PUBLICATIONS AND PRESENTATIONS

1. *Enhancing the Catalytic Properties of Ordered Nanoporous Silicate Using Hydrothermally Treatment Zeolitic Precursors*, Conrad Ingram, Yohannes Ghirmazion, Ifedapo Adeniyi, To be presented at the 57th Southeast/61st Southwest Regional Meeting (November 1-4, 2005).
2. *Synthesis and Catalytic Properties of Hierarchical Mesoporous Aluminosilicate Assembled from Zeolite Y Precursors*; Conrad Ingram, Yohannes Ghirmazion; Ifedapo Adeniyi, to be presented Singapore International Chemical Conference 4, Dec 8-10, 2005
3. *Improved Catalysts for the Heavy Oil Upgrading Based on Zeolite Y Nanoparticles Encapsulated in Stable Nanoporous Host*, Yohannes Ghirmazion and Conrad Ingram, presented at the University Coal Research/HBCU/MIs Contractors' Review Conference, June 7-8 2005, Pittsburgh, Pennsylvania.
4. *Mesoporous Composites from the Sequential Combination of Hydrothermally Treated Colloidal Zeolitic Silicate Precursors*: Yohannes Ghirmazion and Conrad Ingram: submitted to Division of Colloid and Surface Chemistry for the 230th ACS National Meeting, in Washington, DC, Aug 28-Sept 1, 2005 in Washington (from 08-28-2005 to 09-01-2005).
5. *Synthesis of Mesoporous Solids Containing Zeolitic Phase from Hydrothermal Treatment of Colloidal Zeolite Y Precursors* " Yohannes Ghirmazion and Conrad Ingram; to be presented at **Pacificchem 2005**, December 2005.
6. *Zeolites and Other Nanoporous Materials: Synthesis, Characterization and Applications in Fuel Synthesis and Pollution Abatement*; presented at the CAU Chemistry Department's Weekly Seminar, November 9, 2004.
7. *Improved Catalysts for the Heavy Oil Upgrading Based on Zeolite Y Nanoparticles Encapsulated in Stable Nanoporous Host*, Yohannes Ghirmazion and Conrad Ingram, presented at the University Coal Research/HBCU/MIs Contractors' Review Conference, June 7-8 2004, Pittsburgh, Pennsylvania.
8. *Improved Catalysts for the Heavy Oil Upgrading Based on Zeolite Y Nanoparticles Encapsulated in Stable Nanoporous Host*, Yohannes Ghirmazion and Conrad Ingram, presented at the University Coal Research Contractors Review Conference June 3-4 2003, Pittsburgh, Pennsylvania.
9. *Non Ionic Surfactant Mediated Templated Synthesis of Phenylene-Bridged Organosilicate*, Yohannes Ghirmazion*, Conrad Ingram, presented at the 55th Southeast Regional Meeting (SERMACS), Atlanta, GA.

10. *A Comparison of Synthesis Strategies for Arylene Functionalized Ordered Nanoporous Organosilicates using Nonionic and Cationic Surfactants*, Yohannes Ghirmazion*, Conrad Ingram presented at the at the 55th Southeast Regional Meeting (SERMACS), Atlanta, GA.
11. *Catalytic and selective behavior of MeAPO36 in the mild hydrocracking of heavy gas oil*, Conrad W. Ingram, and Kesete Ghebreyessus, Presented at the 227 ACS National Meeting, Anaheim, California
12. *On the Synthesis of Zeolite Y Nanocrystals in the Presence of Tetramethylammonium Bromide*, Yohannes Ghirmazion* and Conrad W. Ingram, presented at the 227 ACS National Meeting, Anaheim, CA.
13. *Phenylene-Bridged Mesoporous Organosilicate from Nonionic Surfactant Templated Synthesis*, Conrad Ingram and Yohannes Ghirmazion, Presented at the 4th International Mesostructured Material Symposium, Cape Tow, South Africa, Extended Abstract 82, Pages 224-225.
14. *Synthesis of Aromatic Bridged Ordered Mesoporous Organosilicate with Cetyltrimethyl-ammonium Cation as Templating Agent*, Conrad Ingram and Yohannes Ghirmazion, Presented at the 4th International Mesostructured Material Symposium, Cape Tow, South Africa, Extended Abstract 86, Pages 231-232.
15. *Studies on the Synthesis of Ordered Mesostructured Aluminophosphates Using Cetyltrimethylammonium Cations as Structure Directing Agents*, C. W. Ingram, S. Abubeker, Inorganic Chemistry Preprints of the 224 ACS Meeting, Boston, MA August 18-22, 2002.
16. *Aluminophosphate Mesostructures from the Hydrolysis and Condensation of Inorganic Precursors*, Sitra Abubekar, **Conrad Ingram** and Jack Eckles Accepted for presentation at NOBCCHE Scientific Conference, New Orleans.
17. *Catalytic and Selective Behavior of MeAPO-36 in the catalytic Cracking of Gas Oil*, Kesete Ghebreyessus and **Conrad Ingram**. *Proceeding of the 13th International Zeolite Conference, 2001, RRR, 26-R-03*
16. *Catalyst Design for the Upgrading of Heavy Oil Under Mild Hydrocracking Conditions*; Kesete Ghebreyessus and **Conrad Ingram**; *6th Historical Black Colleges & Universities/Private Sector/Energy Research and Development Technology Transfer Symposium, MD.*

8. REFERENCES

-
- 1 Petroleum chemistry and refining, J. G. Speight., Taylor and Francis., Washington D.C., 1998.
 - 2 C. Danumah, S.M.J. Zaidi, G.Xu, N. Voyer, S. Giasson, S. Kaliaguine, *Microporous and Mesoporous Materials* 2000 37, p.21.
 - 3 (A) E.M. Flanigen, B. M. Lok, R. L. Patton and S. T. Wilson, *J. Pure and Appl. Chem.*, 58, No. 10, p. 1351.; (B) S.T. Wilson, B.M.Lok, and E.M. Flanigen, U.S. patent 4, 310,440 (1982); S.T. Wilson, B.M. Lok, C. A. Messina, T.R. Cannan, and E.M. Flanigen., *J. Am. Chem.Soc.*, 1982 104, p.1146; (C) B.M. Lok, C.A. Messina, R.L. Patton, R.T. Gajek, T. R. Cannan, and E.M. Flanigen, U.S. patent 4,440, 871 (1984).
 - 4 K. M. Reddy and C. Song, *J. Catalysis Letters*, 1996, p.103.
 - 5 C.T. Kresge, M.E. Leonowicz, W.J. Roth, J.C. Vartuli and J.S. Beck, *Nature*, 1992 359, p.710; S. Beck, J.C. Vartuli, W.J. Roth, M.E. Leonowicz, C.T. Kresge, K.D. Schmitt, C.T.W. Chu, D.H. Olson, D.H. Sheppard, E.W.McCullen, S.B., Higgins, J.B., Schlenker, J. L., *J.Am.Chem.Soc.*, 1992, 114, p.10834.
 - 6 G.D. Stucky, B.F. Chmelka, G.H. Frederickson, Q.Huo, N.W. Melosh, J. Feng, D. Zhao, *Science*, 1998, 279, p.120.
 - 7 A. Sayari, I. Moudrakovski, and J.S. Reddy., *J. Chem. Mater.*, 1996, , p.2080.

-
- 8 Y.Z. Khimiyak, Klinowski., *J. Chem. Soc., Faraday Trans.*, 1998, 94, p. 2241.
 - 9 Y. Yue, Q. Shuiln, L. Shougui, L. Rongsheng, C. Jiesheng, X. Ruren, G. Qiuming, *Faraday Transaction*, 1995, 23, p.310.
 - 10 M.Tiemann and M.Froba., *Chem. Mater.* 1998 10, p. 3475.
 - 11 Oliver, S. Kuperman, A. Coombs, N., Lough, A.Ozin, G.A., J.S., *Nature*, 1995, , p.47.
 - 12 G. Stucky., X. Bu, J. Feng., Y. Xia., P. Feng., *J. Chem. Commun.*, 1997, p. 949.
 - 13 D. Zhao, Z. Luan., L. Kevan, *J. Chem. Commun.*, 1997, p.1009.
 - 14 T. Kimura, Y. Sgahara and K. Kuroda, *J. Chem. Mater.*, 1999, 11, p.508.
 - 15 S. Cabrera, I.E. Haskouri, C. Guillem, A.B. porter, D. B. Porter, S. Mendioroz, M.D. Marcos and P. Amoros., *J. Chem. Commun.*, 1999, p.176.
 - 16 R.F. Mortlock, A.T Bell, C. Radke, *J. Phys.Chem.*, 1993, 97, p.767.
 - 17 R.t Mokaya, *J. Phys. Chem. B.* 2000, 104, p.8275.
 - 18 S. Parsad, Bin Liu-Shang., *J. Chem. Mater.*, 1994, 6, p. 633.
 - 19 R.t Mokaya and W. Jones, *J. Catalysis*, 1997 172, p.211.